The theoretical study of carbon nanostructures

Olga E. Glukhova, DSc, Professor

Saratov State University
Physics Department,
Institute of nanostructures and biosystems

410012, Russia,
Saratov, Astrakhanskaja, 83
E-mail: glukhovaoe@info.sgu.ru

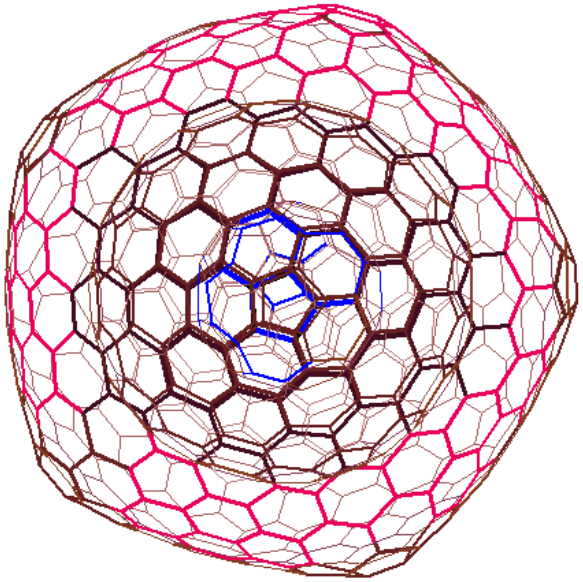

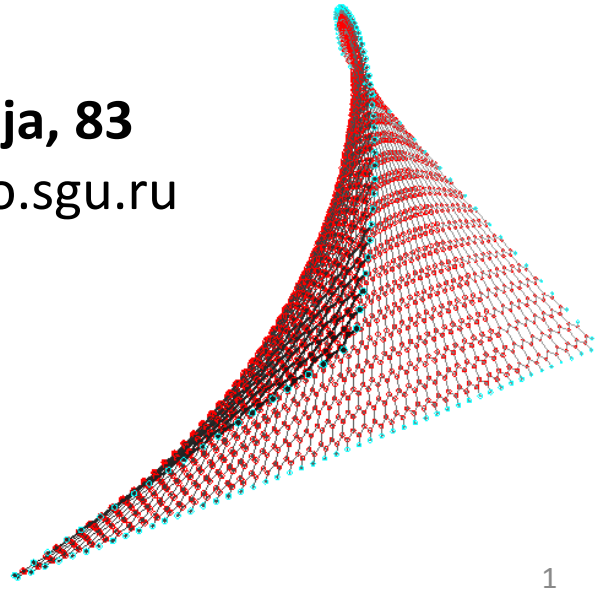

COMPUTATIONAL METHODS: QUANTUM MECHANIC, MOLECULAR DYNAMICS

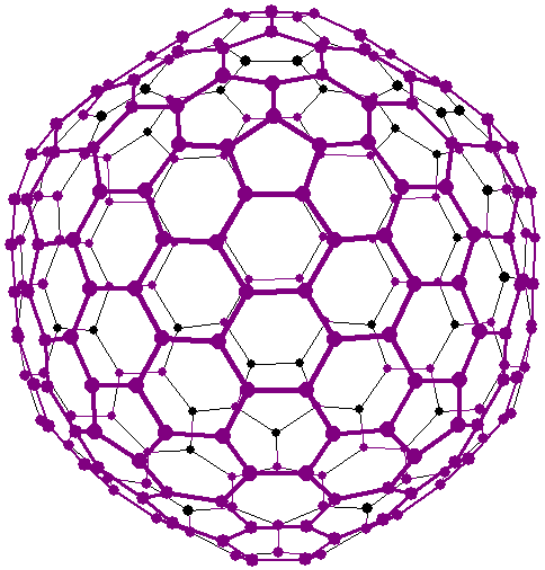

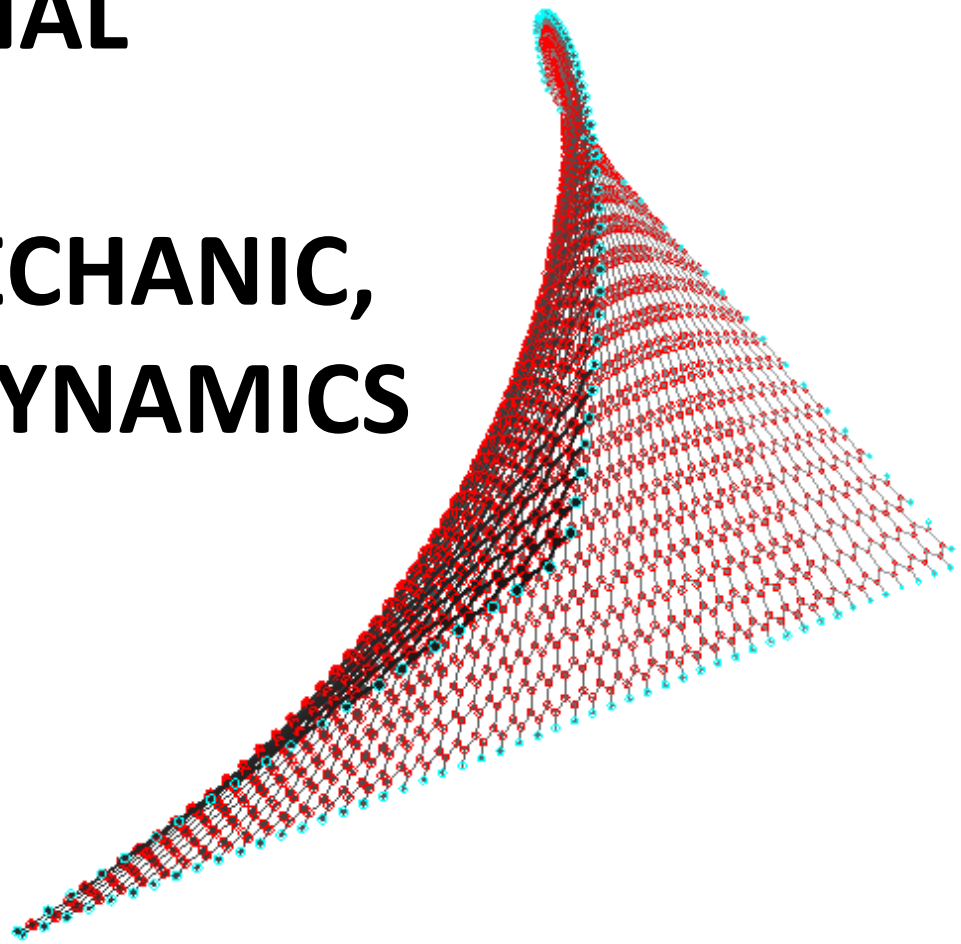

Tight-binding method

The TB method was earlier implemented to study a stability of carbon. The energy of a system of ion cores and valence electrons is written as

$$E_{tot} = E_{bond} + E_{rep}. \qquad (1)$$

Here the term E_{bond} is the bond structure energy that is calculated as the sum of energies of the single-particle occupied states. Those single-particle energies are known by solving the Schrodinger equation

$$\mathbf{H} \mid \psi_n \rangle = \varepsilon_n \mid \psi_n \rangle, \qquad (2)$$

where $\mathbf{H}$ is the one-electron Hamiltonian, ε_n is the energy of the *n*th single-particle state.

The wave functions $|\psi_n\rangle$ can be approximated by linear combination

$$|\psi_n\rangle = \sum_{1\alpha} C_{1\alpha}^n |\varphi_{1\alpha}\rangle, \qquad (3)$$

where $\{\varphi_{1\alpha}\}$ is an orthogonal basis set, l is the quantum number index and α labels the ions.

This approximation is known as the method LCAO – linear combination of atomic orbits.

For example, the one-electron wave function of the compound C_n is given by the combination of the wave functions $|s\rangle, |p_x\rangle, |p_y\rangle, |p_z\rangle$:

$$|\psi\rangle = \sum_{i=1}^{n} c_i |s_i\rangle + \sum_{i=n+1}^{2n} c_i |p_{xi}\rangle + \sum_{i=2n+1}^{3n} c_i |p_{yi}\rangle + \sum_{i=3n+1}^{4n} c_i |p_{zi}\rangle,$$

N is the number of atoms.

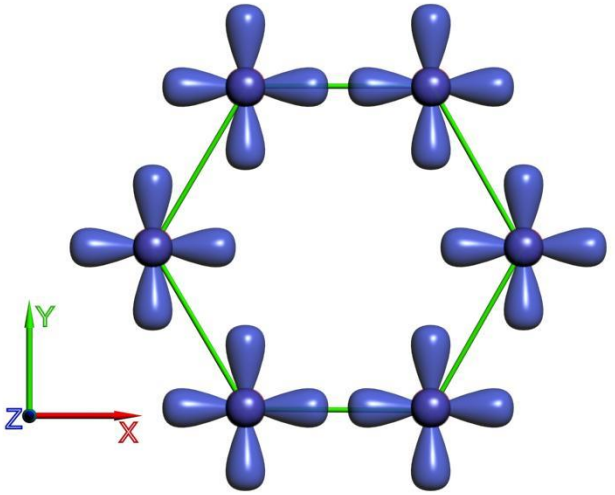

For the tight-binding Hamiltonian, we use the Slater–Koster parameterization scheme for the electronic hopping matrix elements.
The equilibrium hopping integral is

$$V^0_{\alpha\beta} = \langle \varphi_{1'\beta} \,|\, \mathbf{H} \,|\, \varphi_{1\alpha} \rangle.$$

To describe the influence of environment on each atom we have included the scaling function. So, the matrix elements are calculated as (L. Goodwin, A. J. Skinner, and D. G. Pettifor, Europhys.Lett. 9 (1989) 701.)

$$V_{\alpha\beta}(r) = V^0_{\alpha\beta}\left(\frac{p_3}{r}\right)^{p1} \exp\left\{p_1\left[-\left(\frac{r}{p_2}\right)^{p4} + \left(\frac{p_3}{p_2}\right)^{p4}\right]\right\}, \quad (4)$$

where r is the distance between atoms.

The scaling function is known as the function of the two-center TB matrix element between two orbitals of symmetry l and l' placed on the atoms α and β. The parameter p_2 is equal the equilibrium interatomic distance. If the interatomic distance becomes equal the equilibrium distance the function is equal "1".

Once that the single-particle energies are known by solving the secular problem (2).

$$E_{bond} = 2 \sum_{n=1}^{N_{\text{occupied}}} \varepsilon_n$$

Here "2" considers the electron spin.

The phenomenon energy

Term E_{rep} in Eq.(1) is the phenomenon energy that is a repulsive potential. It can be expressed as a sum of two-body potentials as

$$E_{rep} = \sum_{\alpha,\beta\rangle\,\alpha} V_{rep}(r_{\alpha\beta}), \qquad (5)$$

where V_{rep} is pair potential between atoms at α and β. This two-body potential describes an interaction between bonded and nonbonded atoms. The values of the parameters $V^{0}_{\alpha\beta}$, the atomic terms and p_n for carbon compounds are given in table.

The repulsive pair potential is calculated by formula:

$$V_{rep}(r) = p_5\left(\frac{p_3}{r}\right)^{p_6} \exp\left\{p_6\left[-\left(\frac{r}{p_2}\right)^{p_4} + \left(\frac{p_3}{p_2}\right)^{p_4}\right]\right\} \quad (6)$$

All parameters that define the phenomenon energy and were fitted from experimental data for fullerenes and carbon nanotubes.

Transferability to other carbon compounds was tested by comparison with ab initio calculations and experiments. Our parametrization provides the investigations of all modifications of carbon nanostructures. That provides also the study the molecular clusters, finite size structures with sp^2, $sp^{2+\Delta}$, sp^3.

The TB parameters for carbon nanoclusters

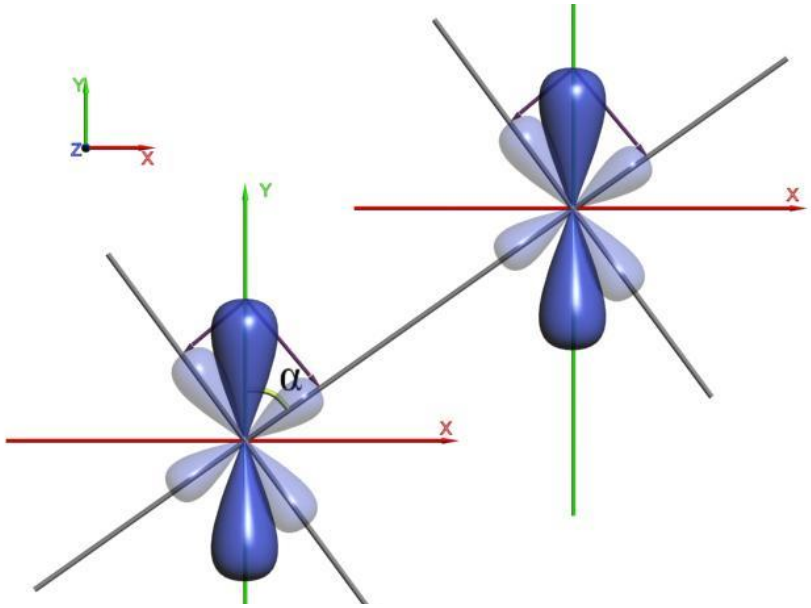

Table 1

ε_s, eV	ε_p eV	$V^0_{ss\sigma}$, eV	$V^0_{sp\sigma}$, eV	$V^0_{pp\sigma}$, eV	$V^0_{pp\pi}$, eV
-10,932	-5,991	-4,344	3,969	5,457	-1,938
p_1	p_2, Å	p_3, Å	p_4	p_5, eV	p_6
2,796	2,32	1,54	22	10,92	4,455

Our transferable tight-binding potential can correctly reproduce changes in the electronic configuration as a function of the local bonding geometry around each carbon atom.

The Hamiltonian

	S_1	S_2	S_3	P_{x1}	P_{x2}	P_{x3}	P_{y1}	…	P_{z3}
S_1	ε_s	$V^0_{ss\sigma}$	$V^0_{ss\sigma}$	0	$V_{sp\sigma}$	$V_{sp\sigma}$	0	…	$V_{sp\sigma}$
S_2	$V^0_{ss\sigma}$	ε_s	$V^0_{ss\sigma}$	$V_{sp\sigma}$	0	$V_{sp\sigma}$	$V_{sp\sigma}$	…	$V_{sp\sigma}$
S_3	$V^0_{ss\sigma}$	$V^0_{ss\sigma}$	ε_s	$V_{sp\sigma}$	$V_{sp\sigma}$	0	$V_{sp\sigma}$	…	0
P_{x1}	0	$V_{sp\sigma}$	$V_{sp\sigma}$	ε_p	V_{pp}	V_{pp}	0	…	V_{pp}
P_{x2}	$V_{sp\sigma}$	0	$V_{sp\sigma}$	V_{pp}	ε_p	V_{pp}	V_{pp}	…	V_{pp}
P_{x3}	$V_{sp\sigma}$	$V_{sp\sigma}$	0	V_{pp}	V_{pp}	ε_p	V_{pp}	…	0
P_{y1}	0	$V_{sp\sigma}$	$V_{sp\sigma}$	0	V_{pp}	V_{pp}	ε_p	…	V_{pp}
…	…	…	…	…	…	…	…	…	…
P_{z3}	$V_{sp\sigma}$	$V_{sp\sigma}$	0	V_{pp}	V_{pp}	0	V_{pp}	…	ε_p

The interaction of P-orbitals

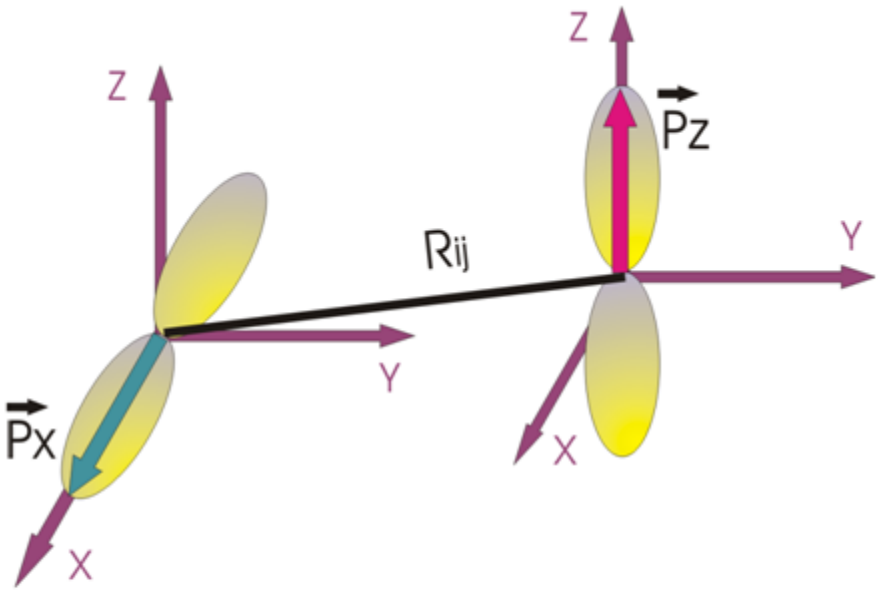

Fig. 1. Schematic representation of the interaction of P_z- and P_x- orbital.

All s- and P-orbitals are given in the real Cartesian co-ordinates system. To correctly reproduce changes in the electronic configuration of the local bonding geometry around each atom we have defined P-orbital as the axial vector. Each axial vector makes the angle with an direction R_{ij} (α, β, θ) and may be written as the geometrical sum of the two vectors:

$$\vec{P}_x = \vec{P}_{xD} + \vec{P}_{x\perp}, \vec{P}_y = \vec{P}_{yD} + \vec{P}_{y\perp}, \quad (7)$$
$$\vec{P}_z = \vec{P}_{zD} + \vec{P}_{z\perp}.$$

Here $\vec{P}_{xD}$, $\vec{P}_{yD}$, $\vec{P}_{zD}$ are projections to an iteratomic direction, $\vec{P}_{x\perp}$ ... are projections to an orthogonal direction.

So, to describe the interaction between P_z and P_x (see Fig.) we must write:

$$\vec{P}_x \cdot \vec{P}_z = \underbrace{\vec{P}_{xD} \cdot \vec{P}_{zD}}_{\sigma\text{-bonding}} + \underbrace{\vec{P}_{x\perp} \cdot \vec{P}_{z\perp}}_{\pi\text{-bonding}}. \quad (8)$$

Angle between projections $\vec{P}_{xD}$ and $\vec{P}_{zD}$ is equal to zero, but an angle between projections to an orthogonal direction is not zero and it is equal to γ (see Fig.). As a result of some mathematical transformations we can write the expressions for cosγ and the energy of the interaction between P_z and P_x:

$$\cos\gamma = -\frac{\cos\alpha\cdot\cos\theta}{\sin\alpha\cdot\sin\theta}, \qquad (9)$$

$$V_{PxPz}(r_{ij}) = V^{\sigma}_{PxPz}(r_{ij})\cdot\cos\alpha\cdot\cos\theta + V^{\pi}_{PxPz}(r_{ij})\cdot\sin\alpha\cdot\sin\theta\cdot\cos\gamma =$$

$$= V^{\sigma}_{PxPz}(r_{ij})\cdot\cos\alpha\cdot\cos\theta + V^{\pi}_{PxPz}(r_{ij})\cdot\sin\alpha\cdot\sin\theta\cdot\left(-\frac{\cos\alpha\cdot\cos\theta}{\sin\alpha\cdot\sin\theta}\right) =$$

$$= \cos\alpha\cdot\cos\theta\left(V^{\sigma}_{PxPz}(r_{ij}) - V^{\pi}_{PxPz}(r_{ij})\right) \qquad (10)$$

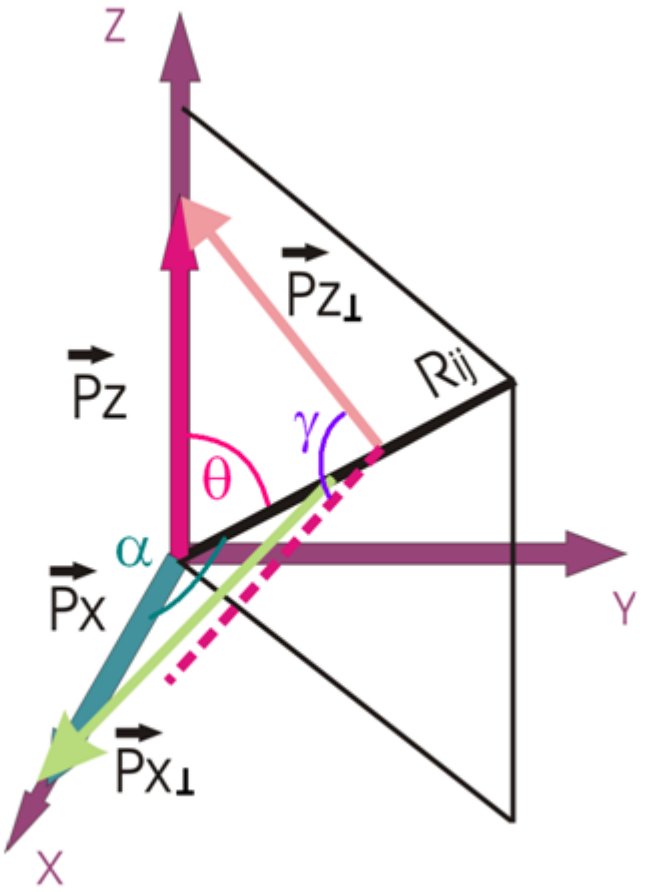

Fig. 2. Projections *of P_z- and P_x- vectors.*

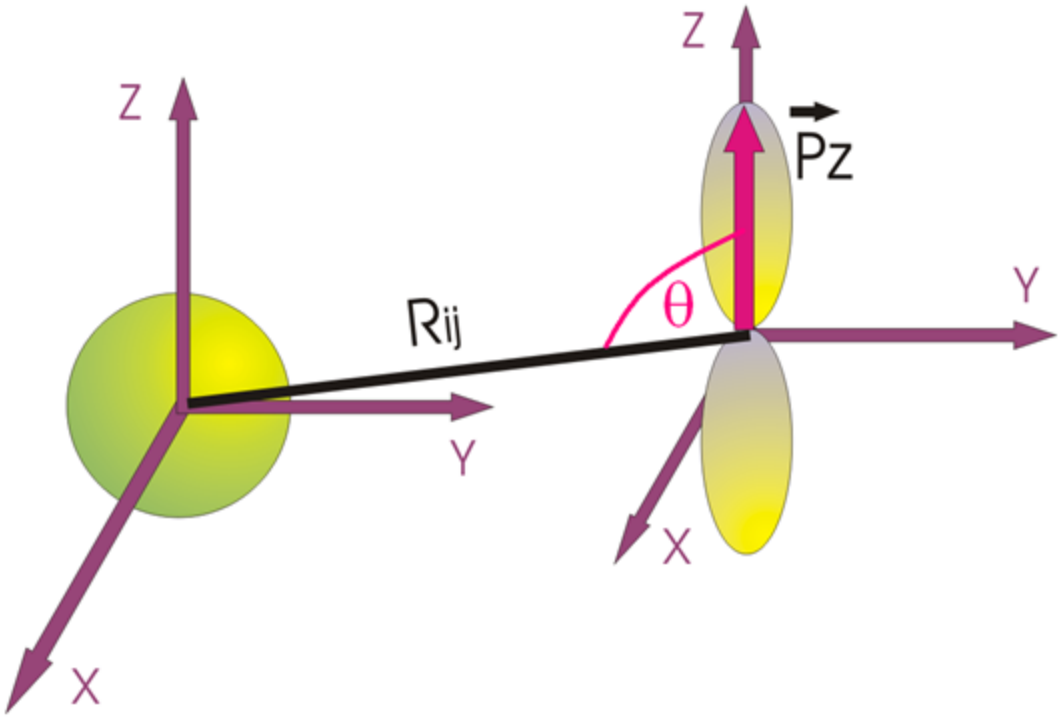

Fig. 3. Schematic representation of the interaction of P_z- and S- orbitals.

As well known, the expression for the energy of the interaction between S and P-orbitals can be defined very simple:

$$V_{SPz}(r_{ij}) = V^{\sigma}_{SPz}(r_{ij}) \cdot \cos\theta \qquad (11)$$

The rehybridization

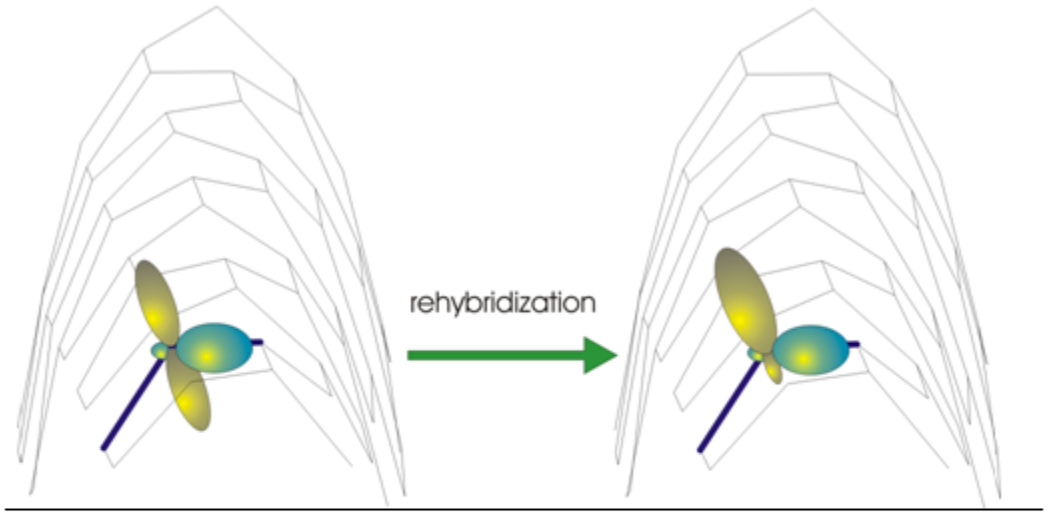

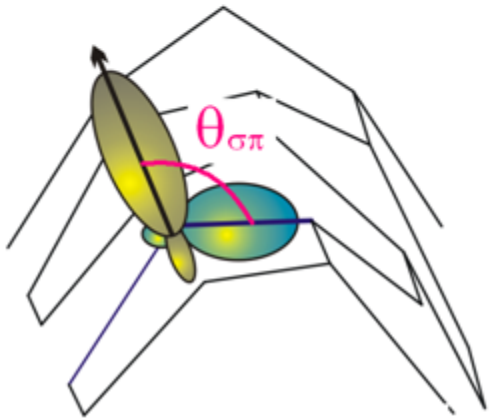

Presented scheme to reproduce the electronic configuration and the local bonding geometry around each atom provides the consideration and calculation of the rehybridization between σ- and π-orbitals. In Figure 4 we can see that the atom is in sp^2 hybridization becomes that in $sp^{2+\Delta}$ hybridization because of a curvature of the topological network.

Degree of rehybridization is defined on the pyramidalization angle. This angle is calculated on formula:

$$\theta_p = \theta_{\sigma\pi} - \pi/2.$$

Angle $\theta_{\sigma\pi}$ is presented as shown in Fig. 4. π-orbital axis vector makes equal angles to the σ-bonds at a conjugated carbon atom.

The electron spectra

So, the presented transferable tight-binding potential and the described scheme to reproduce the electronic configuration and the local bonding geometry around each atom are well suited for computer simulations of covalently bonded systems in both gas-phase and condensed-phase systems.

We have tested our scheme by comparison with experiments for fullerene and some carbon nanotubes. In the table the spectra of the π-orbitals and density of states are presented.

Results are inresonable agreement with experimental data.

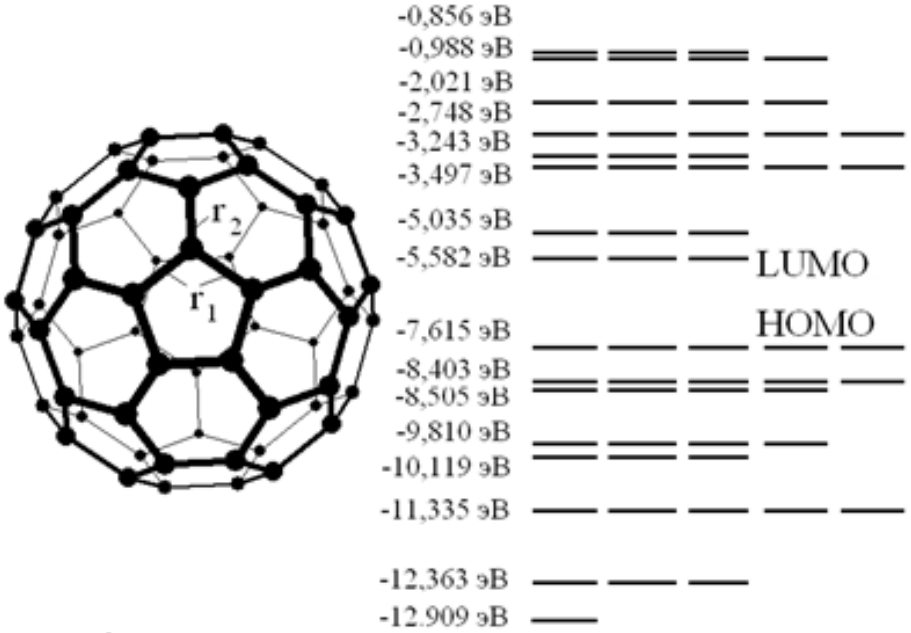

Fullerene C_{60} and the spectra of π-orbitals

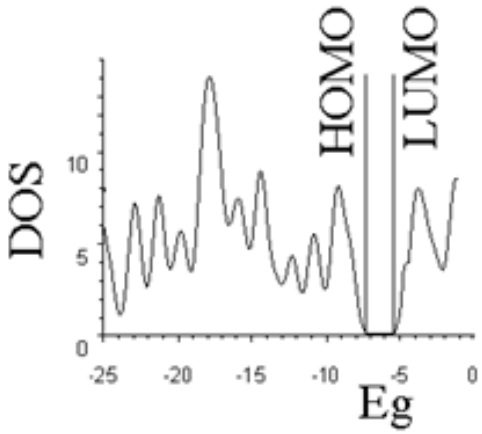

IP = 7.61 eV, Eg = 2 eV

r_1 = 1.45 A, r_2 = 1.40 A.

To describe the intermolecular interaction the van der Waals potential was added in to the system energy (1). The van der Waals potential is given as the Lennard-Jones potential

$$E_{vdW} = \sum_{\alpha,\beta\rangle\alpha} \frac{A}{\sigma^6}\left(\frac{1}{2}y_0^6 \frac{1}{\left(r_{\alpha\beta}/\sigma\right)^{12}} - \frac{1}{\left(r_{\alpha\beta}/\sigma\right)^{6}}\right), \qquad (12)$$

where $\sigma = 1.42$ is a length of the C-C bond, $y_0 = 2.7$ and $A = 24.3 \cdot 10^{-79}\ J \cdot m^6$ are empirically chosen parameters (Qian D., Liu W. K., and Ruoff R. S. (2003) C. R. Physique 4: 993-100). However, the Lennard-Jones potential is incorporated only if the phenomenon intermolecular energy becomes zero (at distance about 0.25 nm for the carbon-carbon interaction).

The motions of the atoms are determined by the classical MD method where Newton's equations of motion are integrated with a third-order Nordsieck predictor corrector. Time steps of 0.15–0.25 fs were used in the simulations. The forces on the atoms were calculated using TB method.

To research the nanoribbons using tight-binding potential our own program was used. Our own program provides the calculation of the total energy of nanostructures, which consist of 500-5000 atoms. We have adapted our TB method to be able to run the algorithm on a parallel computing machine (computer cluster).

During consideration of the algorithm we can note two points:

solution of eigenvalues problem and, possibly, eigenvectors problem for the M*NxM*N matrix - one-electron Hamiltonian (N is the number of atoms, M is maximum number of valence electrons);

- solution of optimization problem – the total system energy minimization.

It's necessary to consider the available computing power.

We have a number of dual-processor servers which are the distributed SMP-system. MPI (stands for Message Passing Interface) was chosen as mechanism for implementing parallelism.

Nanoreactor (nanoautoclave)

Dimerization of miniature C_{20} and C_{28} fullerenes in nanoautoclave

NANODEVICES: MATHEMATICAL MODELS

In our nanoautoclave model a closed single-wall carbon nanotube (10,10) C_{740} is represented as a capsule that is closed from both ends with C_{240} fullerene caps. The pressure is controlled by a shuttle-molecule encapsulated into a nanotube that may move inside the tube. In the present case a shuttle-molecule is the C_{60} fullerene. The shuttle must have some electric charge for its movement to be controlled by an external electric field. The positively charged endohedral complex $K^+@C_{60}$ (the ion of potassium inside the fullerene C_{60}) is a shuttle-molecule in the present model of the nanoautoclave. So, the hybrid compound $K^+@C_{60}@tubeC_{740}$ is a nanoautoclave model. The $K^+@C_{60}@tubeC_{740}$ nanoparticle is located between two electrodes connected with a power source. Changing the potentials at the electrodes, we control the movement of the $K^+@C_{60}$ fullerene.

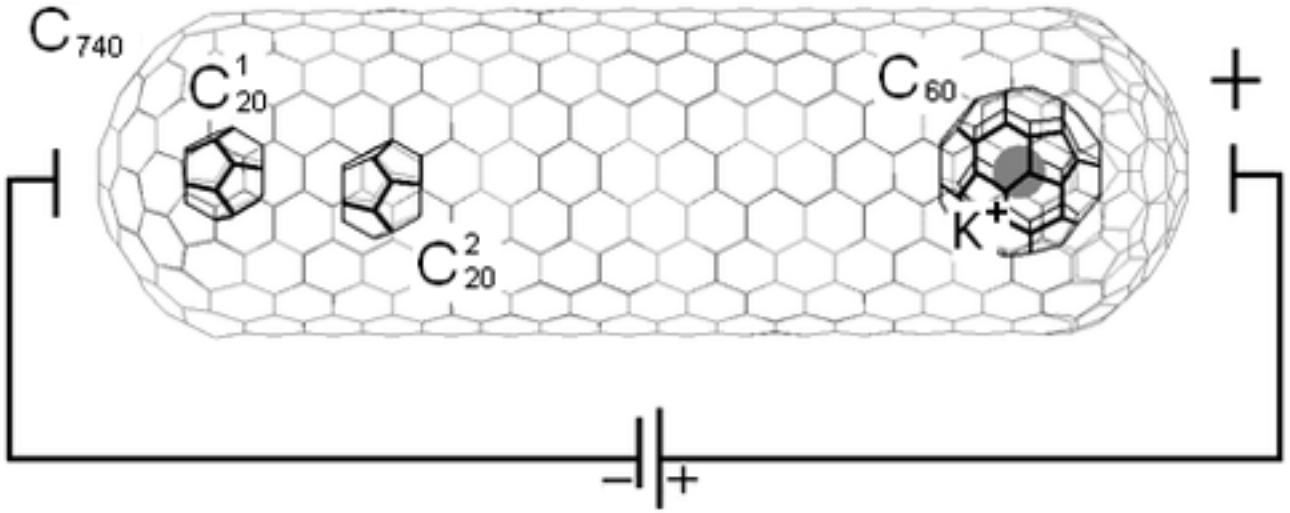

At the start moment, the mutual positions of all nanoautoclave components correspond to the ground state

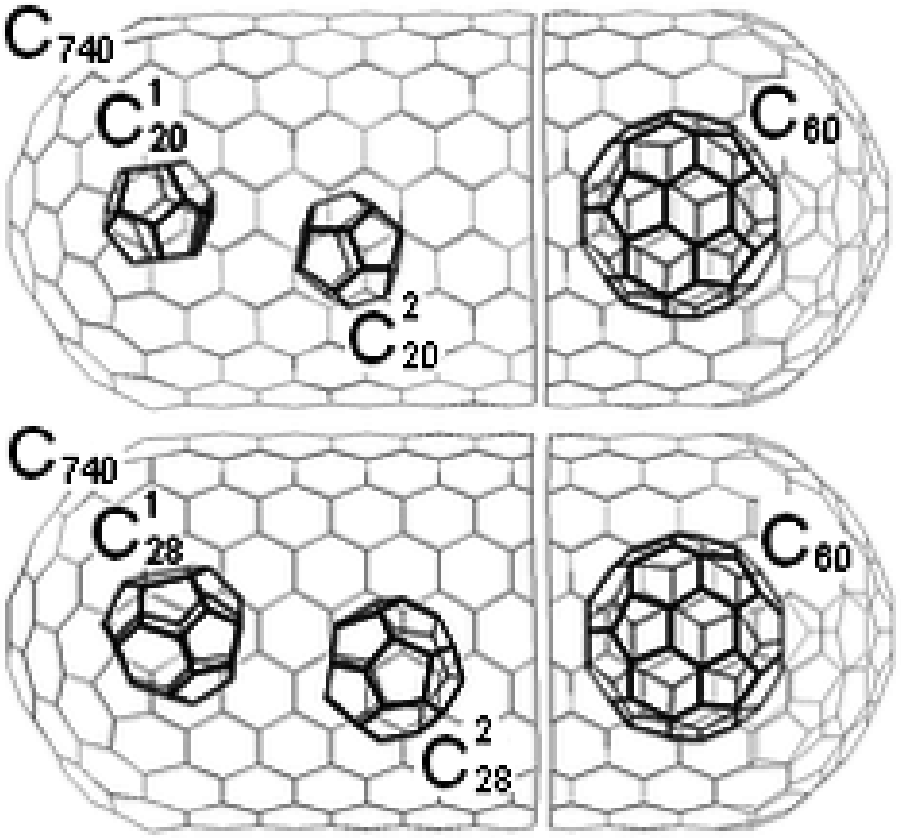

When the pressure created in the tube provides both the overlap of π-electrons of the C_n fullerenes (that corresponds to the interatomic distance of about 1.9 Å) and the covalent bonds formation, the intermediate phase of the $(C_n)_2$ dimer is synthesized: $(C_{20})_2$ $[5+5]$ (at $n=20$) or $(C_{28})_2$ $[6+6]$ (at $n=28$). Here a number of fullerene atoms participating in the intermolecular bonds formation is shown in square brackets. Figure shows a stable dimer of the C_{20} (C_{28}) fullerene and the C_{60} molecule that suffered a certain deformation.

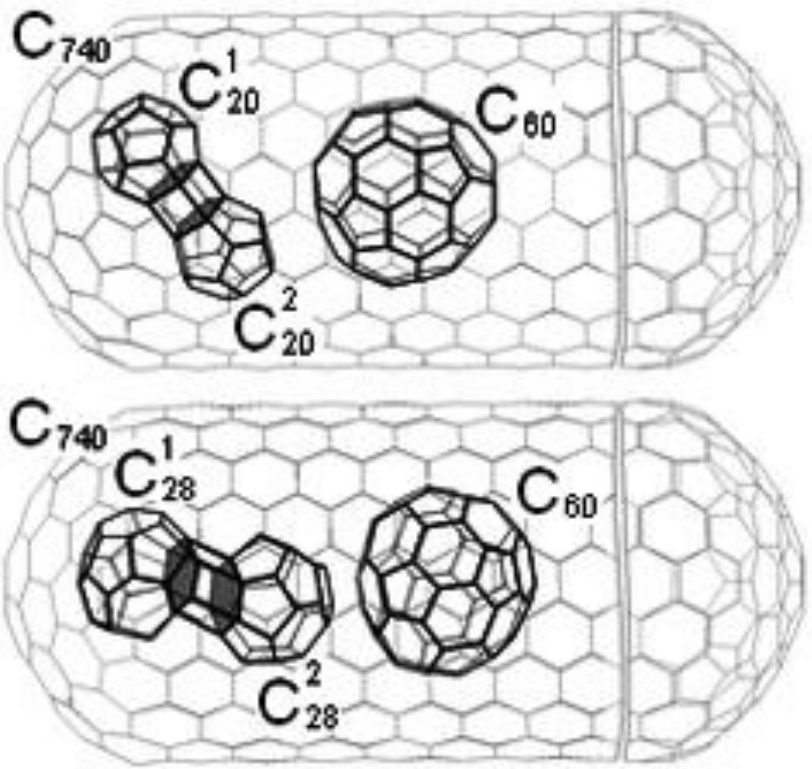

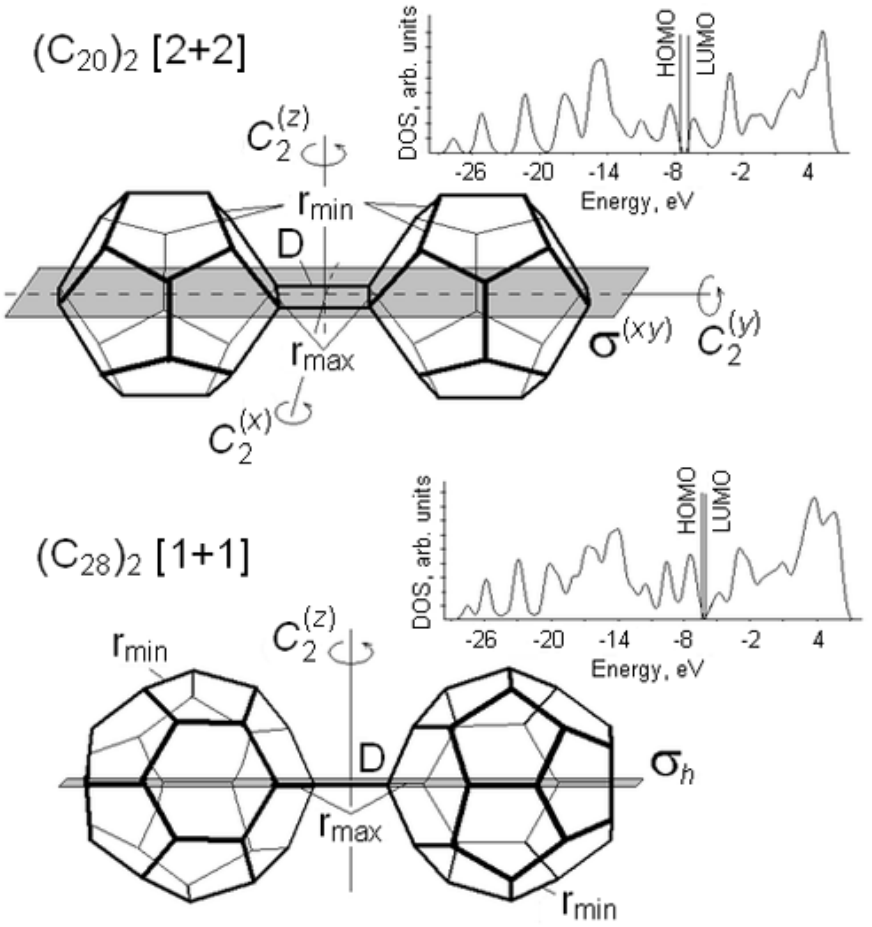

The structure of stable dimers with the horizontal symmetry plane, symmetry axes, and the plot of electron states density are shown in Figure.

Characteristics of stable fullerenes dimers

Dimer	Symmetry group of the dimer	r_{min}/r_{max}, Å	D, Å	E_b, eV	ΔH, $\frac{kcal}{mol \cdot atom}$	E_g, eV	HOMO, eV
$(C_{20})_2[2+2]$	D_{2h}	1.43/1.62	1.65	6.44	-5.01	0.66	7.00
$(C_{28})_2[1+1]$	C_{2h}	1.41/1.56	1.56	6.57	-2.07	0.14	7.16

At the moment of the covalent bonds formation, the pressure is calculated according to the energy $E_{inter} = E_{vdW} + E_{rep}$. The potential difference at the electrodes $\Delta\varphi$ that provides the pressure necessary for the dimerization is calculated according to the relationship $\Delta E_{inter} = e \cdot \Delta\varphi$, where ΔE_{inter} is a potential barrier overcome by the C_{60} fullerene when it goes from the well (the area of the tube end) to the position providing the dimer formation. The strength is calculated as $\Delta\varphi / L$, where a distance L is taken to be equal to the capsule length added to value of 3.4 Å (closing the capsule to electrodes by a less distance may cause sticking due to Van-der-Waalse interaction).

The energy of the C_{60} fullerene and parameters of the outer field necessary for the $(C_n)_2$ dimer synthesis

$(C_n)_2$	$E_{inter}(1)$, eV	ΔE_{inter}, eV	$\Delta\varphi$, V	F, V/m
$(C_{20})_2[2+2]$	-3.574	5.42	8.90	$0.18 \cdot 10^8$
$(C_{28})_2[1+1]$	-3.574	6.50	10.16	$2 \cdot 10^8$

Graphene: electron properties

With increasing of the number of atoms the nanoribbon becomes stable (finite size effect)

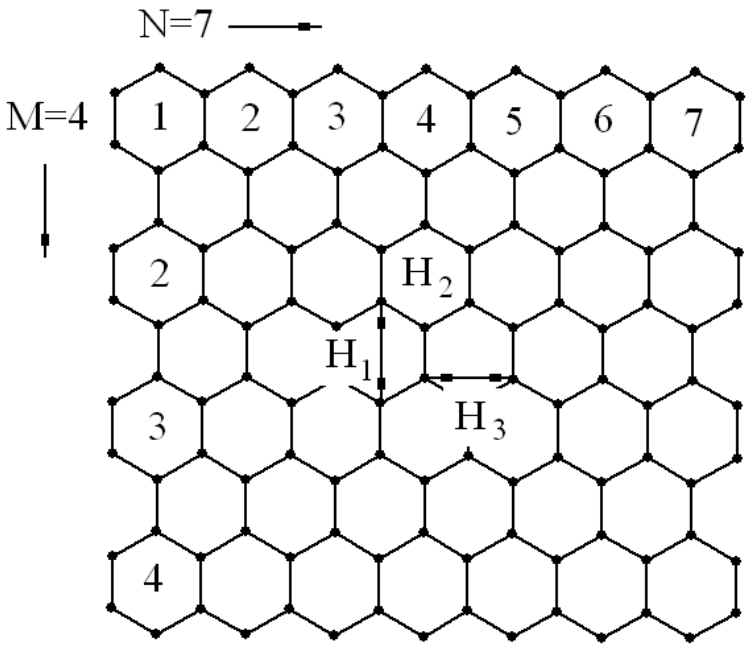

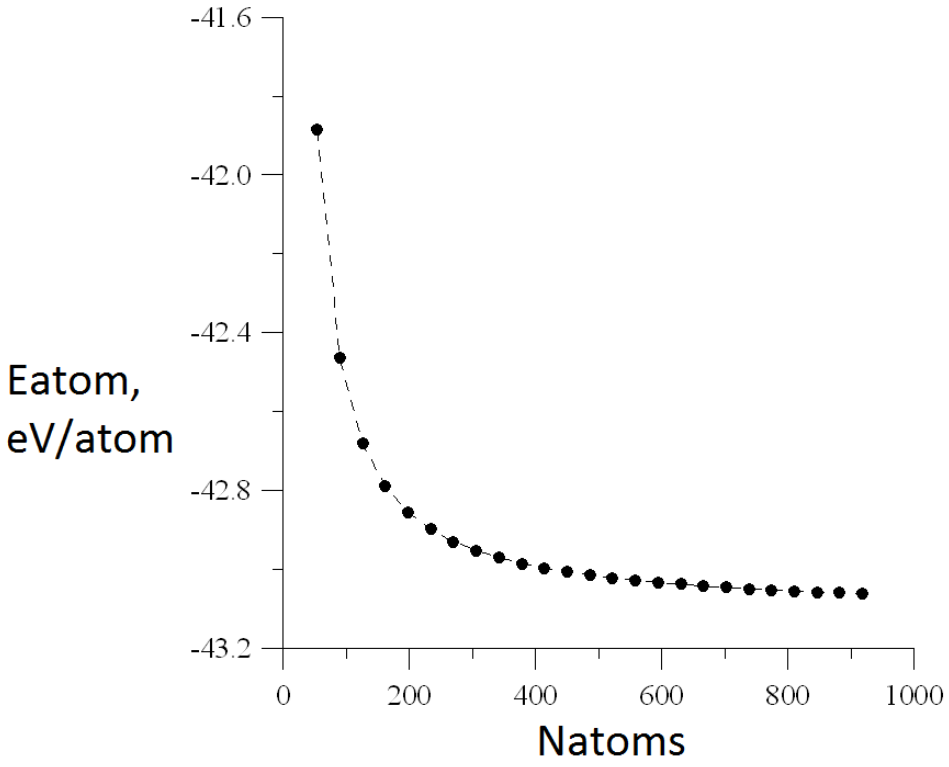

Density of Mulliken charge of carbon atoms of nanoribbon

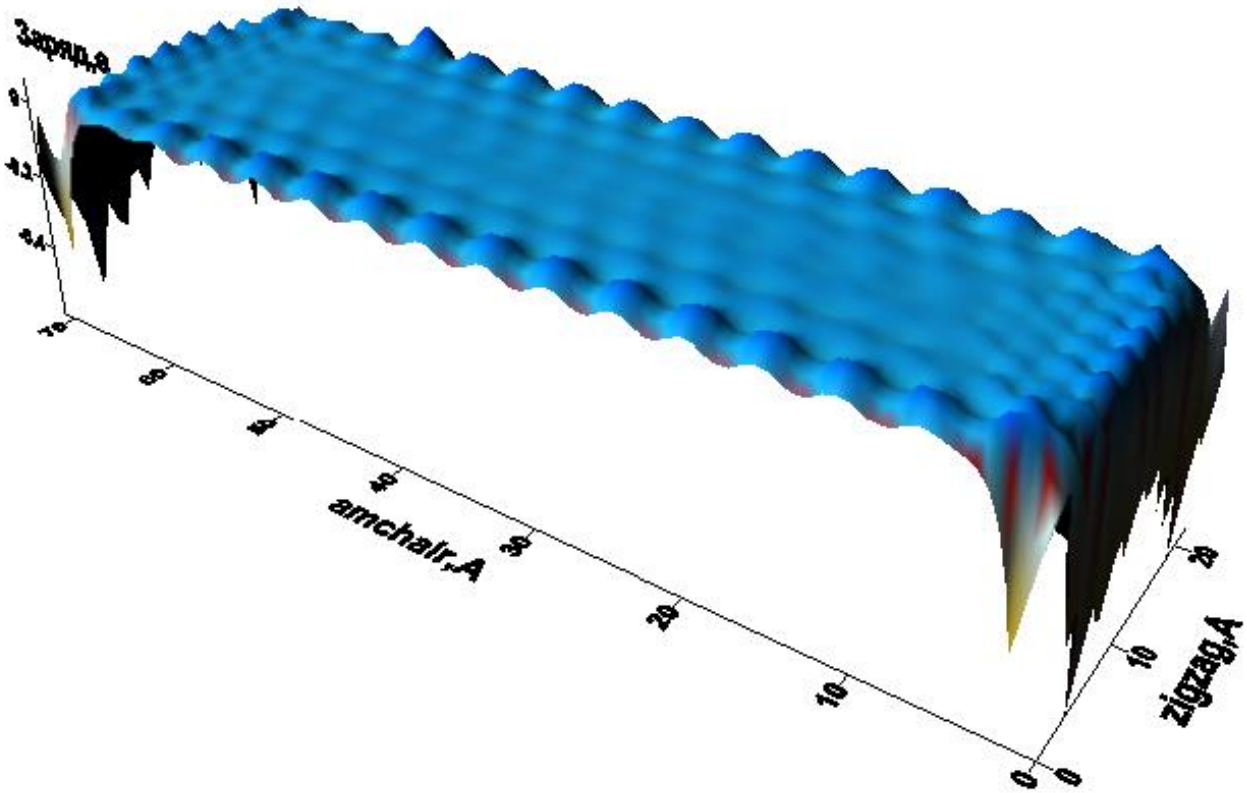

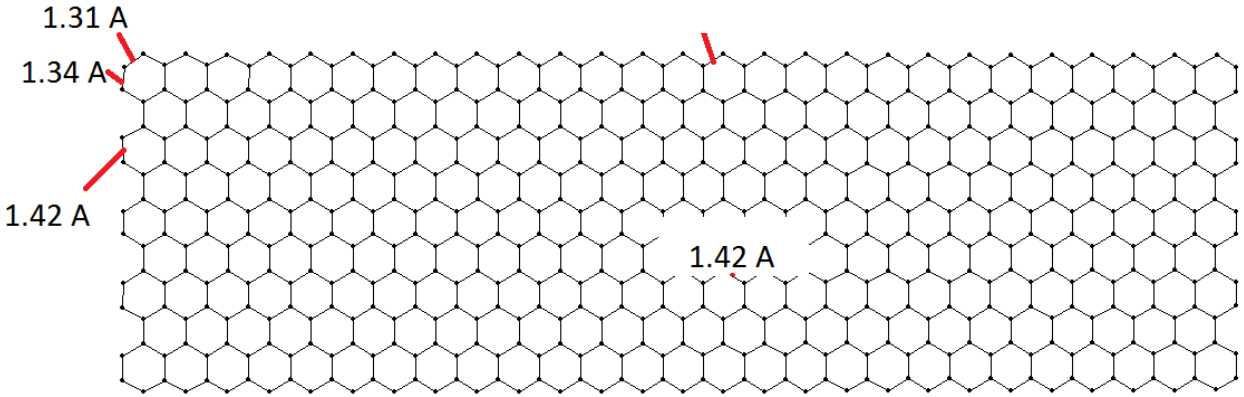

Scroll of nanoribbon (finite size effect)

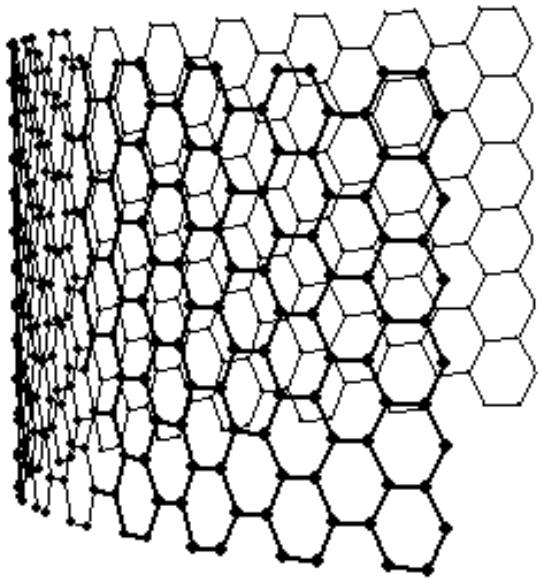

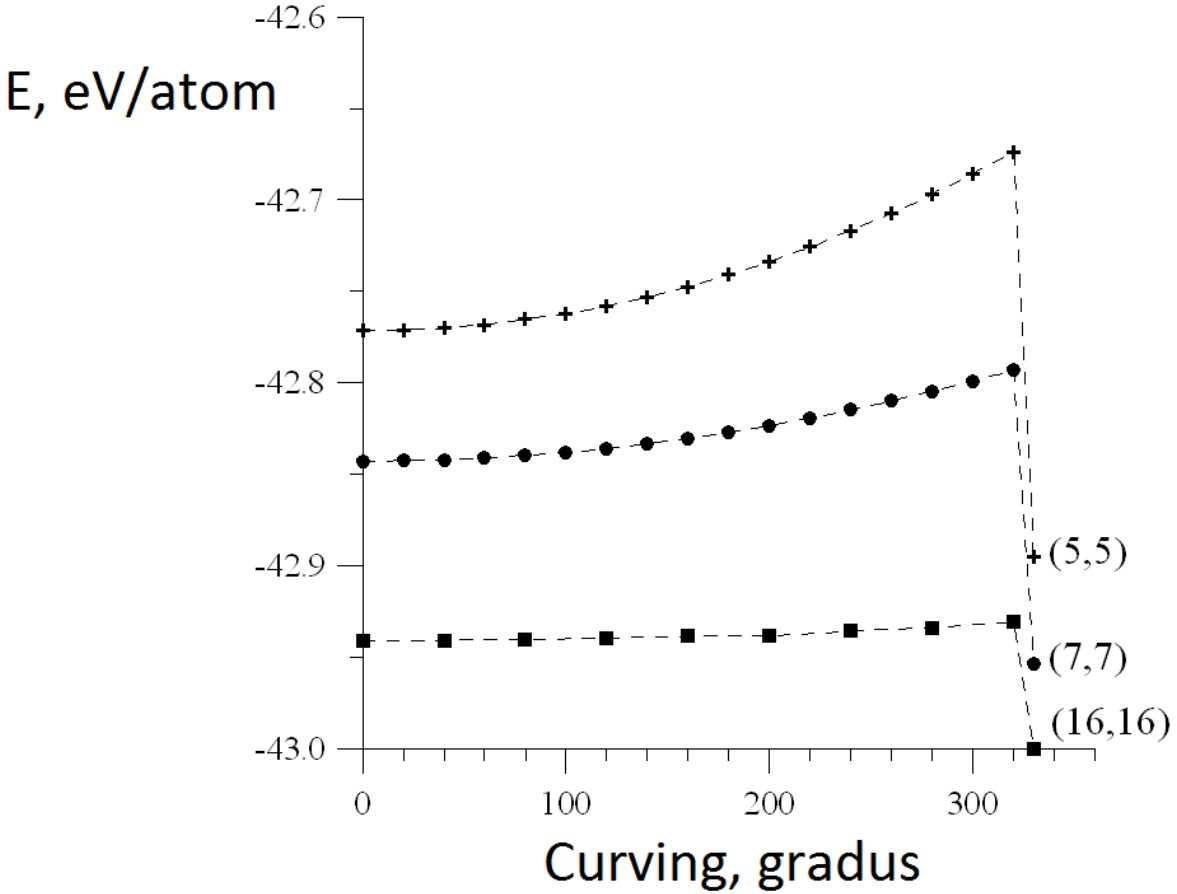

The dependency of IP on the nanoribbon length (finite size effect)

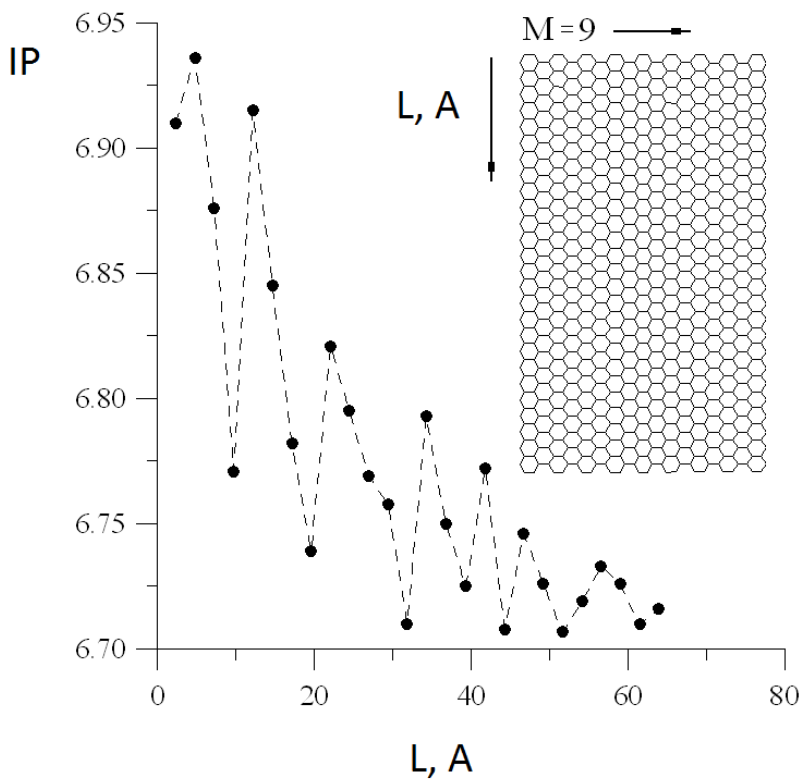

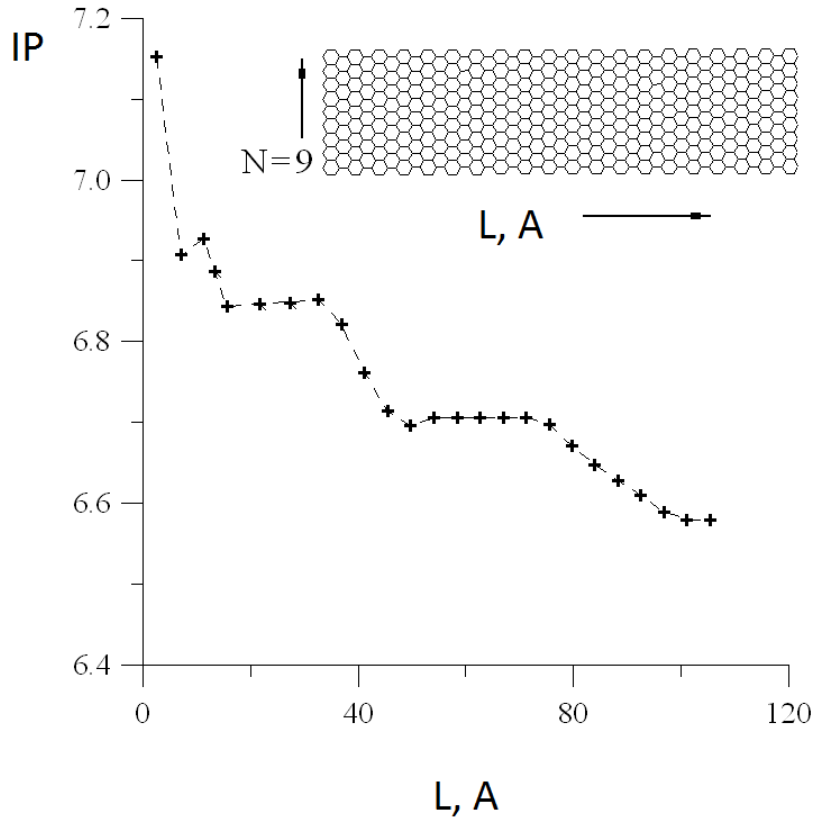

IP of nanoribbons

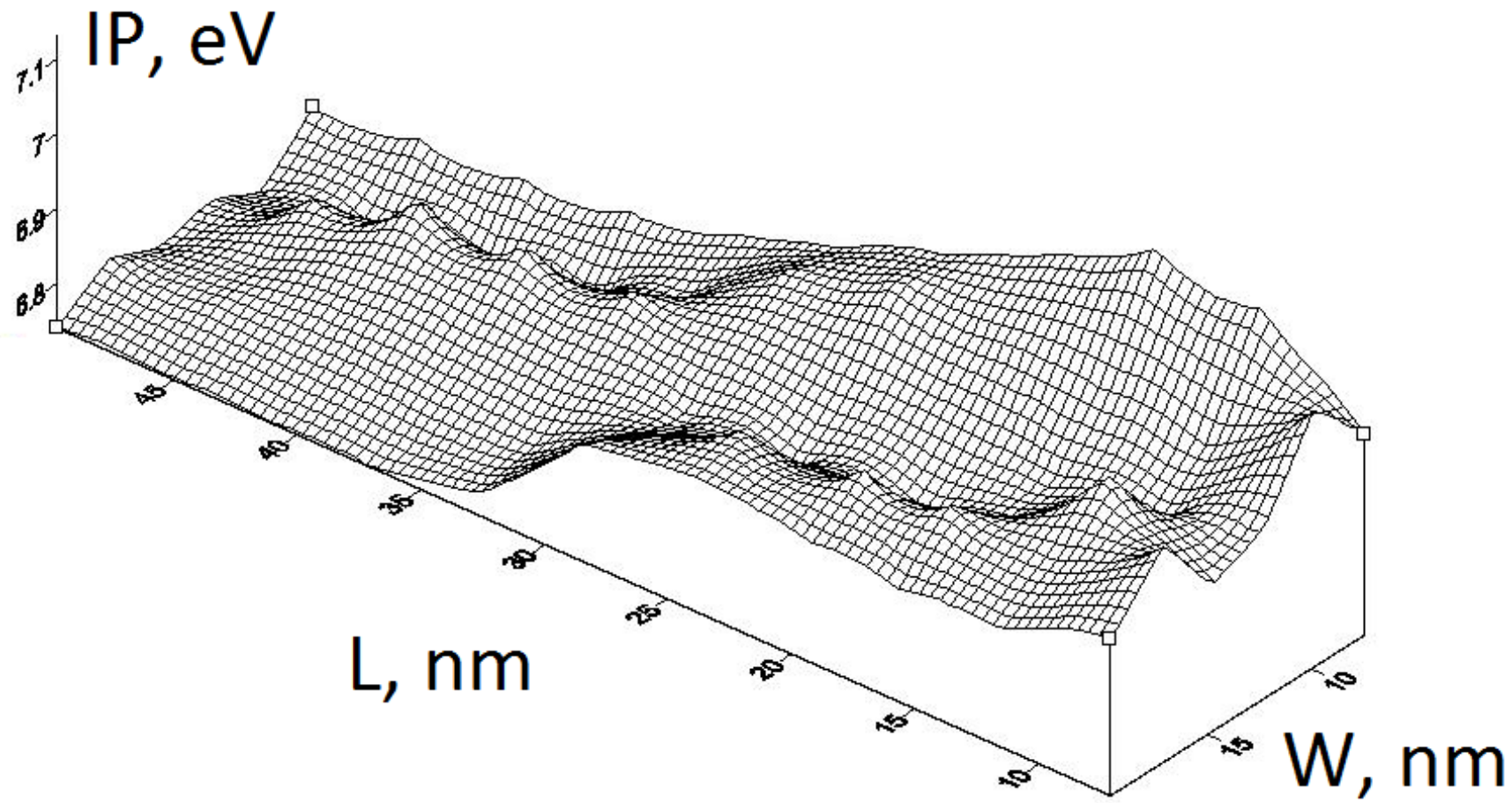

Energy gap of nanoribbons

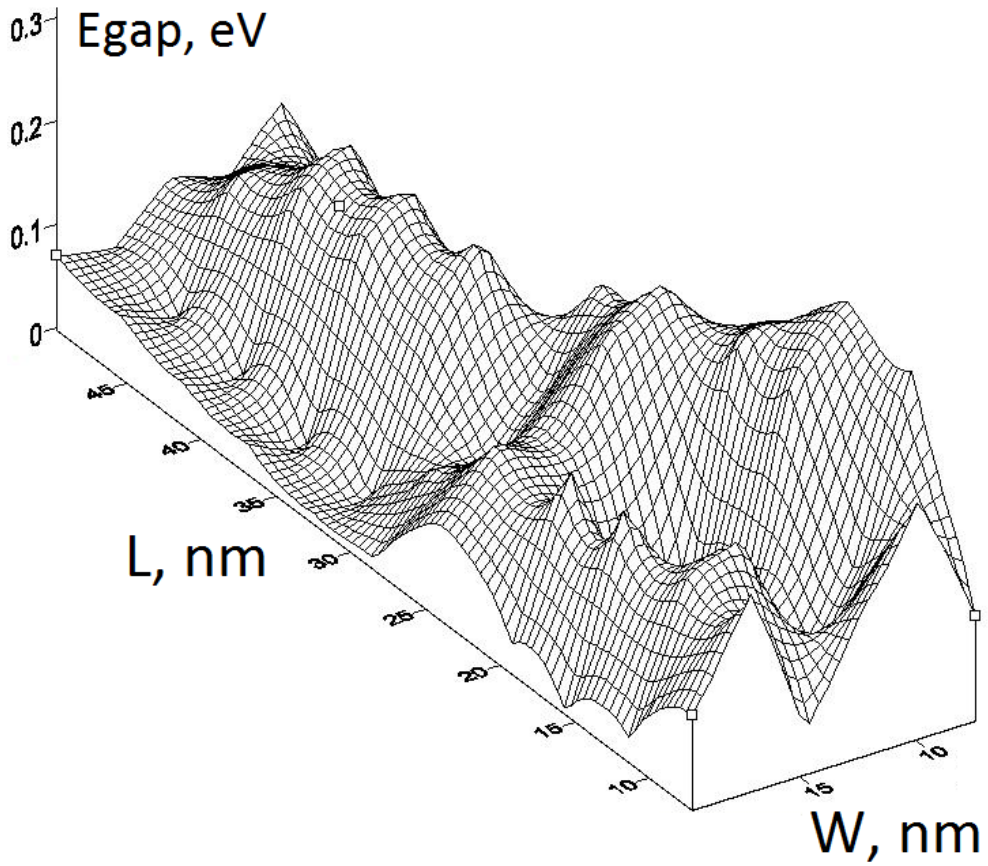

Defected nanoribbons

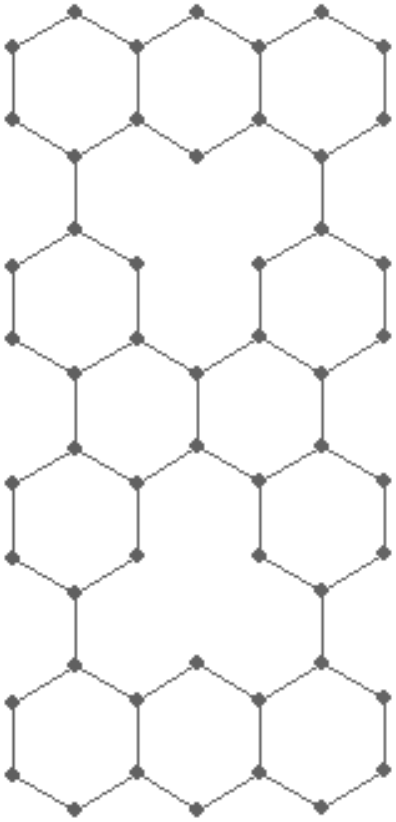

The dependency of IP on the concentration of defect

	0 %	1,8 %	3,6 %	5,4 %
IP, eV	7,15	7,11	7,14	7,15

The dependency of the energy gap on the concentration of defect

	0 %	1,8 %	3,6 %	5,4 %
Egap, eV	0,28	0,14	0,07	0,03

GRAPHENE: MECHANICAL PROPERTIES

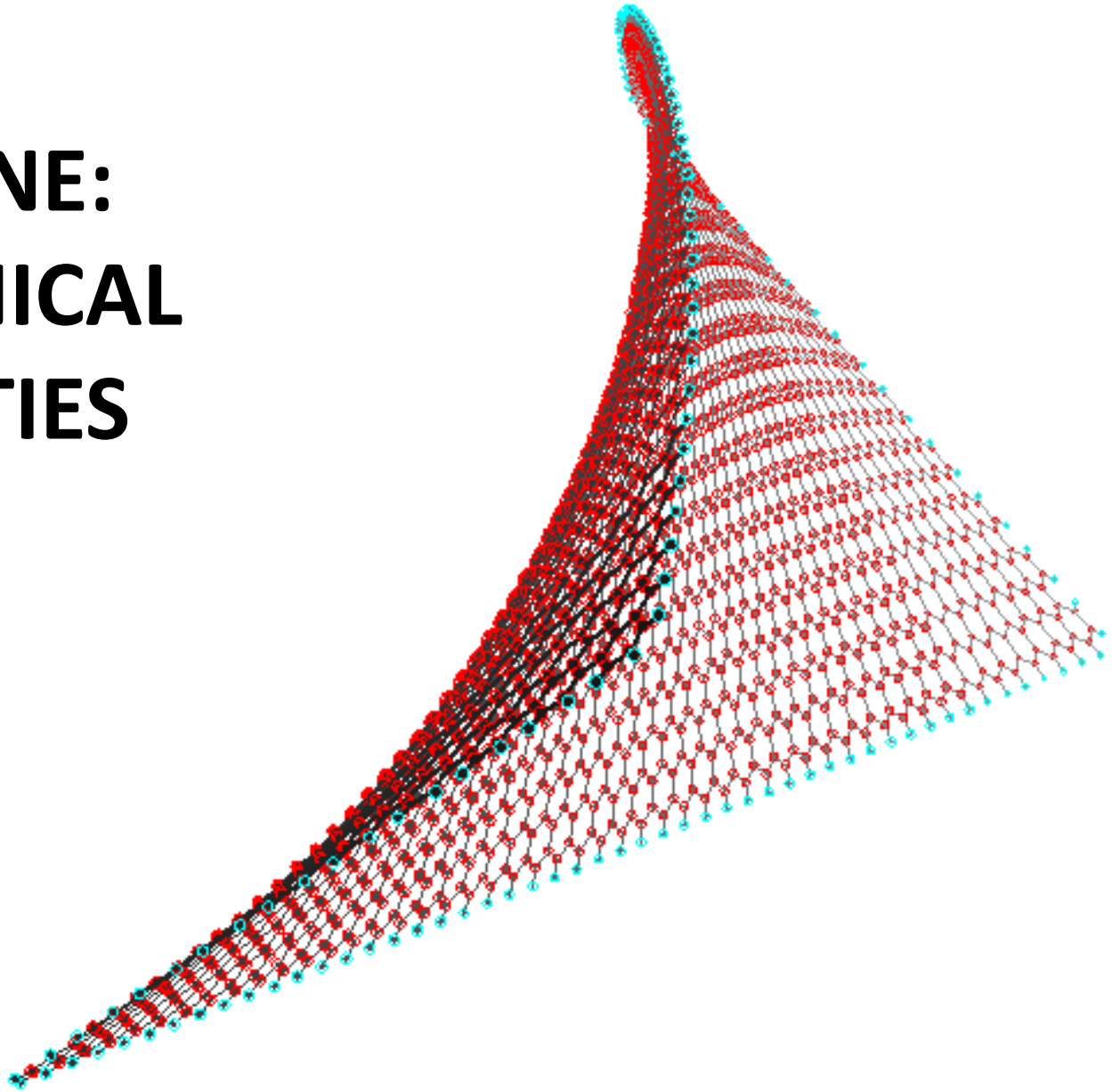

Multicsale modeling to investigate the mechanical properties

Deformations and elastic properties: empirical study

Computational method

The entire system energy is described by the sum of the binding energy E_b, the torsional energy E_{tors} and the van der Waals energy E_{vdW}:

$$E_{tot} = E_b + E_{tors} + E_{vdW}. \quad (1)$$

In order to study the elastic properties and deformations of graphene-graphane nanoribbons we applied the empirical method based on the bond-order potential developed by Brenner.

To describe the interaction between the atom and its environment we introduce three different regions in topological network (see Figure 1). As shown in Fig.1, there are near (first), far (third) and intermediate (second) regions about an atom with number i. Atoms from the near region are covalently bonded with the atom i, atoms from other regions are non-bonded with this atom. The far region has no borders.

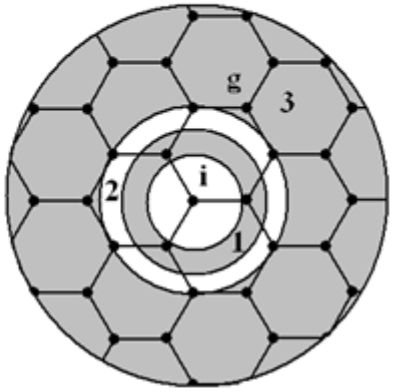

Fig. 1. Three different regions in topological network of an atomic structure

Each pair of covalently bonded atoms interacts via a potential-energy:

$$E_b = \frac{1}{2}\sum_{i=1}^{Nat}\left(\sum_{j(\neq i)}\left(V_R(r_{ij}) - B_{ij}\,V_A(r_{ij})\right)\right). \quad (2)$$

This is the binding energy. Here V_R is the repulsive pair term, V_A is the attractive pair term, r_{ij} is the distance between the atom with number i and atom j from near region. The function B_{ij} is the many-body term. This term was introduced to describe the specificity of the σ–π interaction. So, the value of the binding energy depends on the position and chemical identity of atoms.

The torsional potential is given by the formula

$$E^{tors} = \frac{1}{2}\sum_{i=1}^{Nat}\left(\sum_{j\neq i}\left(\sum_{k\neq i,j}\left(\sum_{l\neq i,j,k} V_{tors}(\omega_{ijkl})\right)\right)\right). \quad (3)$$

The torsional potential $V_{tors}(\omega_{ijkl})$ is given as a function of a dihedral angle ω. The torsion angle ω_{ijkl} is defined in the usual way as the angle between the plane defined by the vectors $\mathbf{r}_{ik}$ and $\mathbf{r}_{ij}$ and that defined by $\mathbf{r}_{ij}$ and $\mathbf{r}_{jl}$. Here atoms j and k are given from intermediate (second) region and the atom l is given from far region.

Van der Waals energy E_{vdW} defines the interaction between non-bonded atoms:

$$E_{vdW} = \frac{1}{2}\sum_{i=1}^{Nat}\left(\sum_{j(\neq i)} V_{vdW}(r_{ij})\right). \quad (4)$$

Van der Waals interaction energy may be described by the Lennard-Jones, Morse, Buckingham potentials and so on. We have implemented and compared Lennard-Jones and Morse potentials as the functions to define the van der Waals energy. We use Morse potential that is given by

$$V_{Morse}(r_{ij}) = D_e\left(\left(1-\exp\left(-\beta(r_{ij}-r_e)\right)\right)^2 - 1\right) + E_r \cdot \exp\left(-\beta' r_{ij}\right), \quad (5)$$

where D_e is the average bond energy, E_r is the repulsion nucleus energy, β, β' - parameters.

Study of deformations and elastic properties of nanoparticles and nanoribbons was implemented on the following algorithm

1) Optimization of atomic structure by entire system energy minimization on atomic coordinates (the atomic structure obtained from previous optimization);
2) Tension or compression of the atomic network of nanoribbon and reoptimization of atomic structure with fixed atoms on the nanoribbon ends;
3) Calculation the Young's pseudo-modulus for the elastic tension of nanoribbon on 1% on formula:

$$Y_p = \frac{F}{D}\frac{L}{\Delta L}$$

where a deformation force is given by $F = \frac{2\Delta E}{\Delta L}$. Here ΔE is the strain energy, namely, the total energy at a given axial strain minus the total.

4) Calculation the Young's modulus for the elastic tension of nanoribbon on 1% on formula:

$$Y = \frac{F}{S}\frac{L}{\Delta L}$$

Young's pseudo-modulus (Y^{2D}) of nanoribbons. $Y^{3D} = Y^{2D} * 0.34$ nm

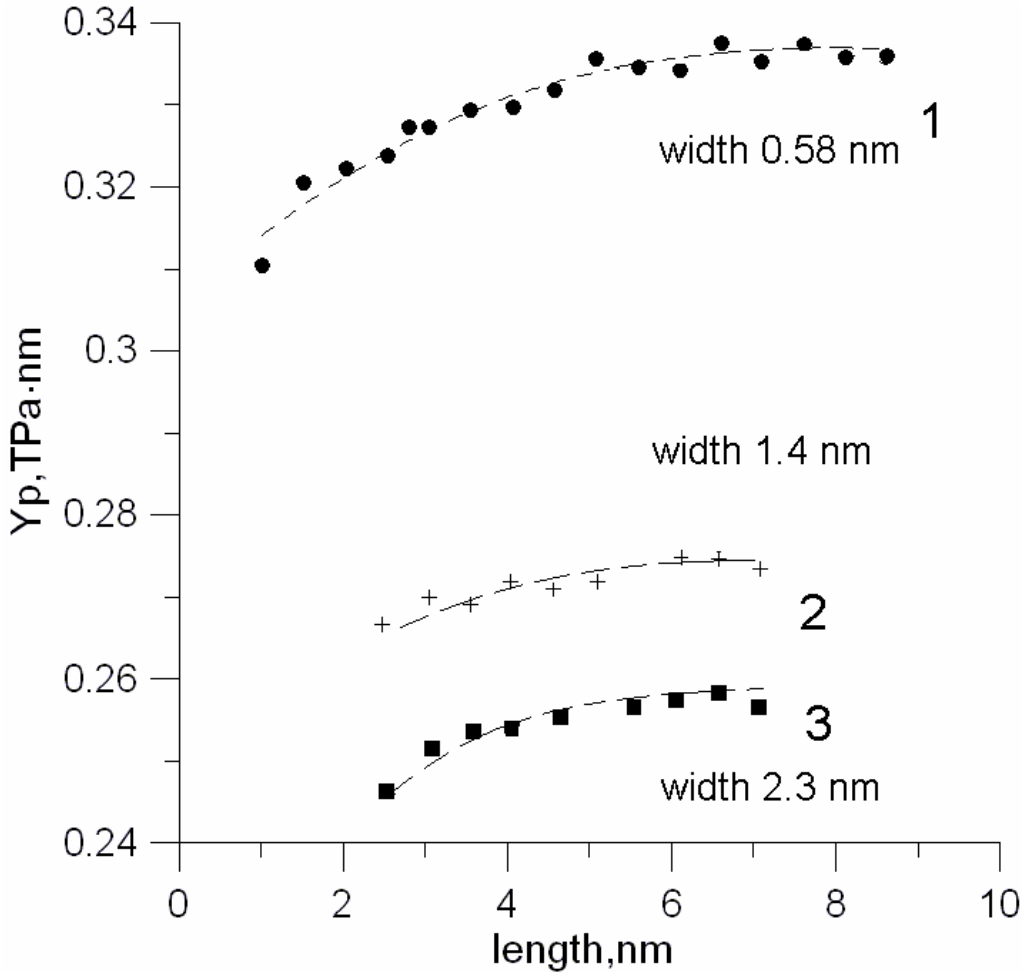

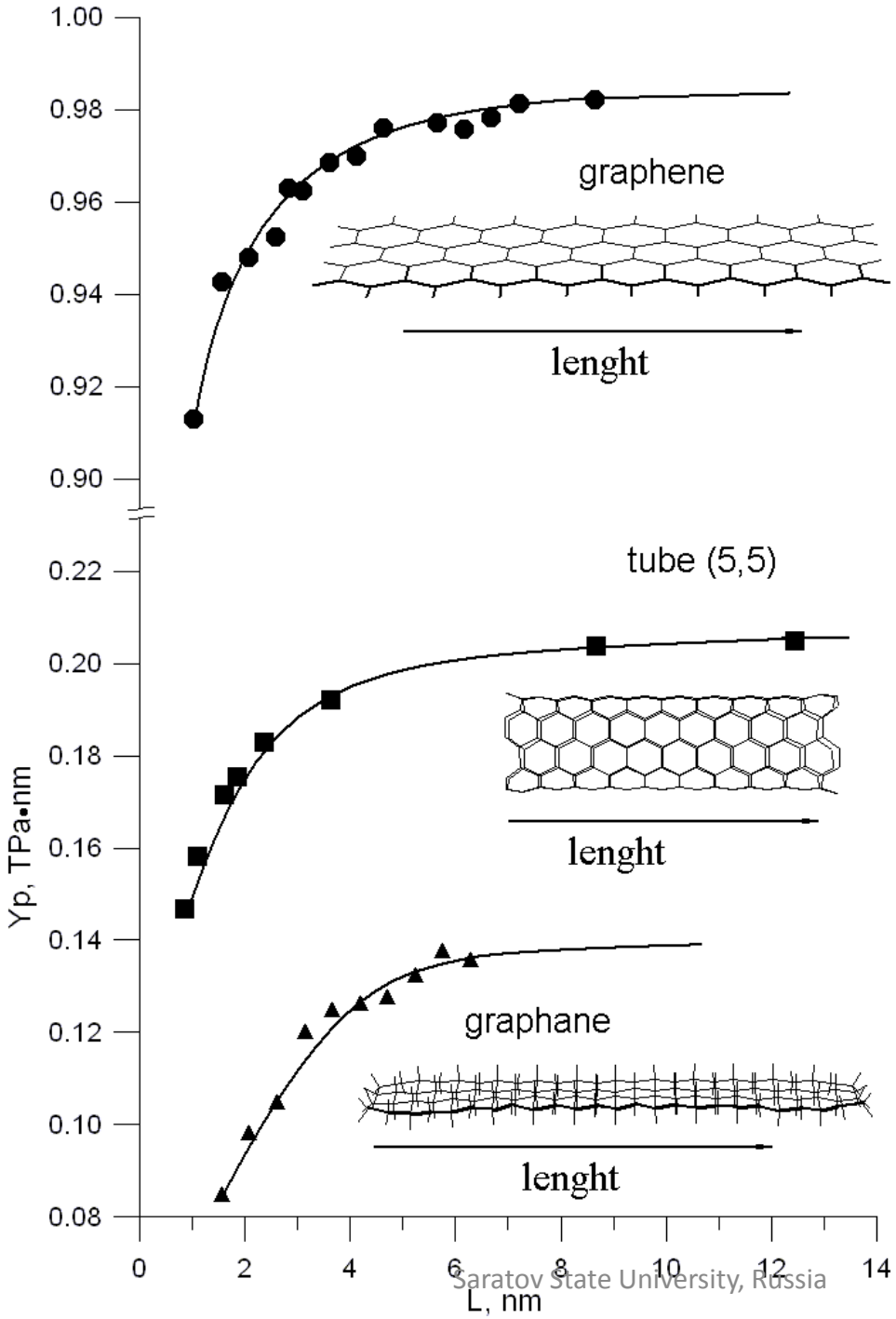

Two-dimensional Young's modulus

Strain energy of nanoribbons undergoing axial tension

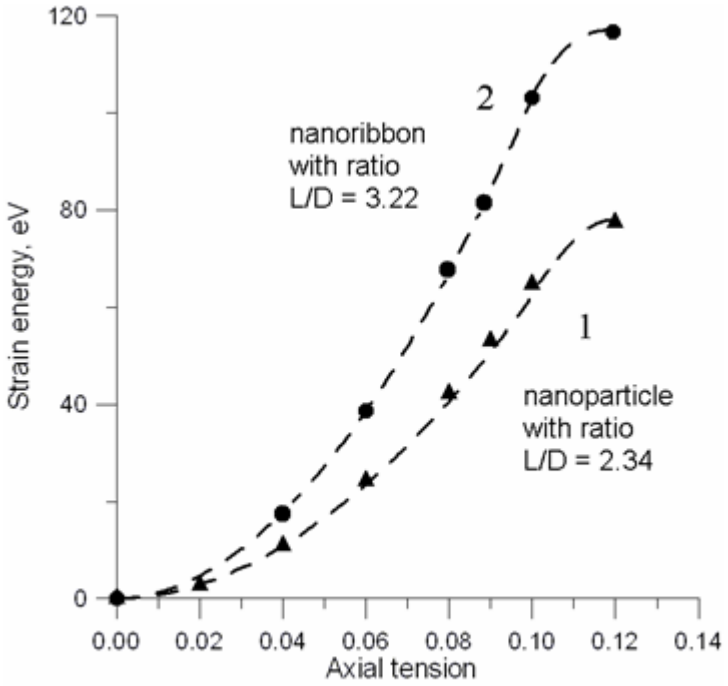

a) Armchair-nanoribbons

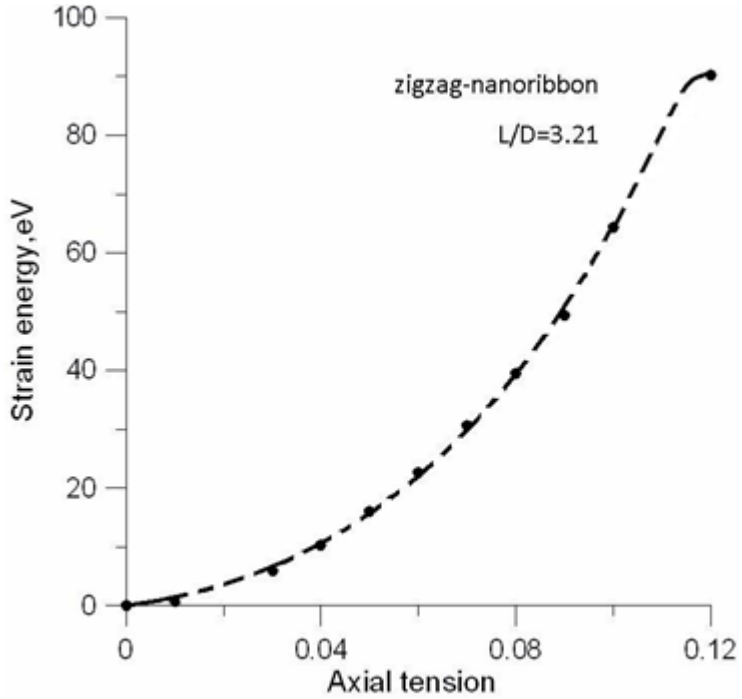

b) Zigzag-nanoribbons

Nanoribbon undergoing axial compression

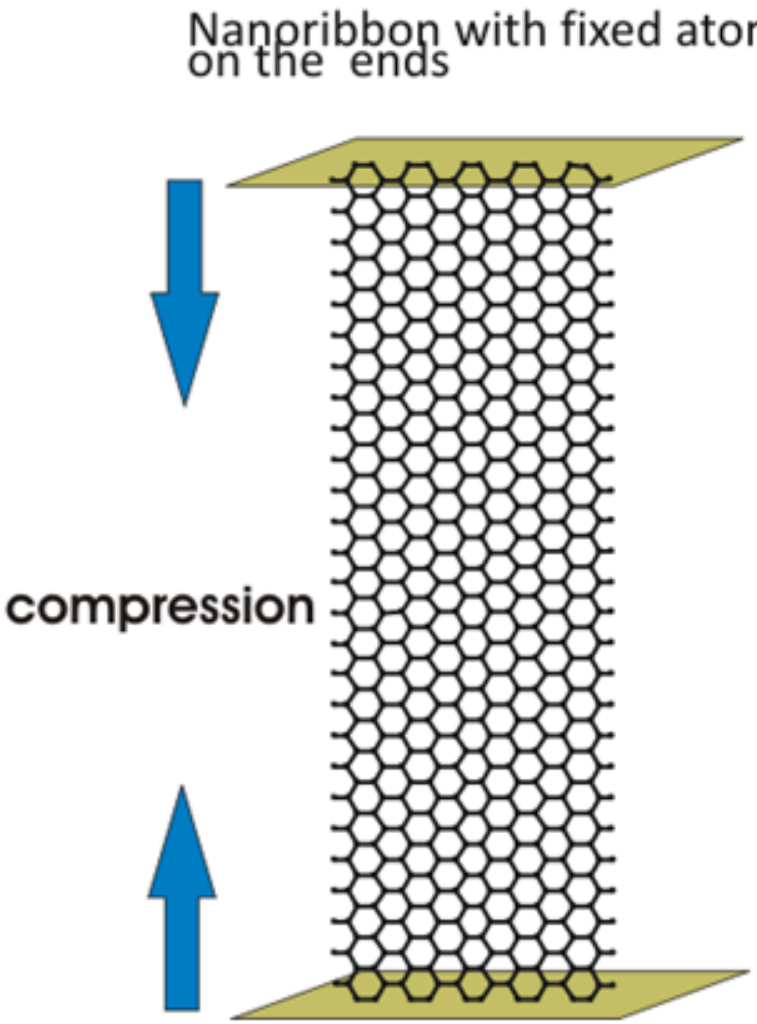

Atoms on the ends were fixed on the plates. The plates were moved to wards each other to decrease the length for some percent.

Dependence of strain energy on the relative compression nanoribbons

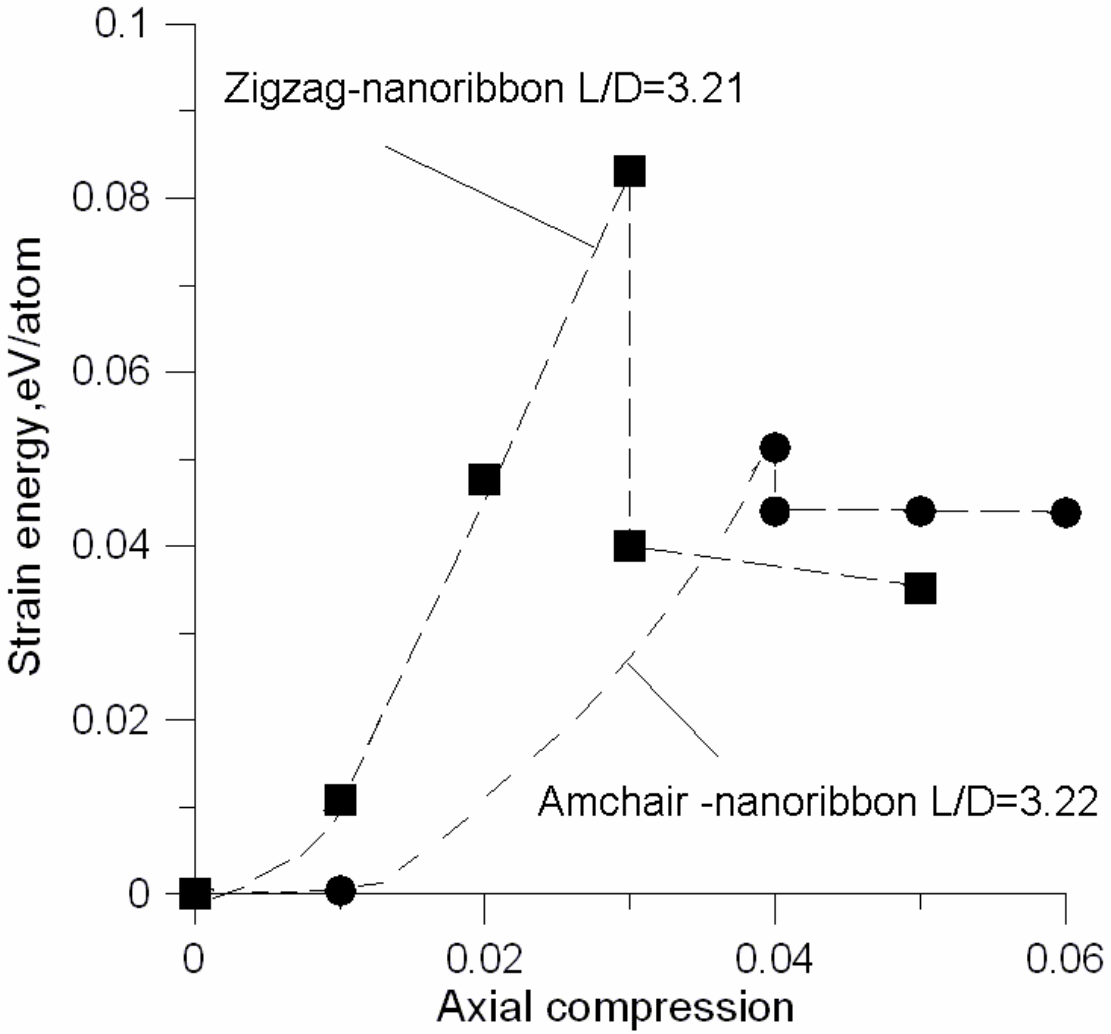

The curve of the strain energy collapse occurs at the axial compression 0.03-0.04. Plane atomic network undergoing axial compression becomes wave-like.

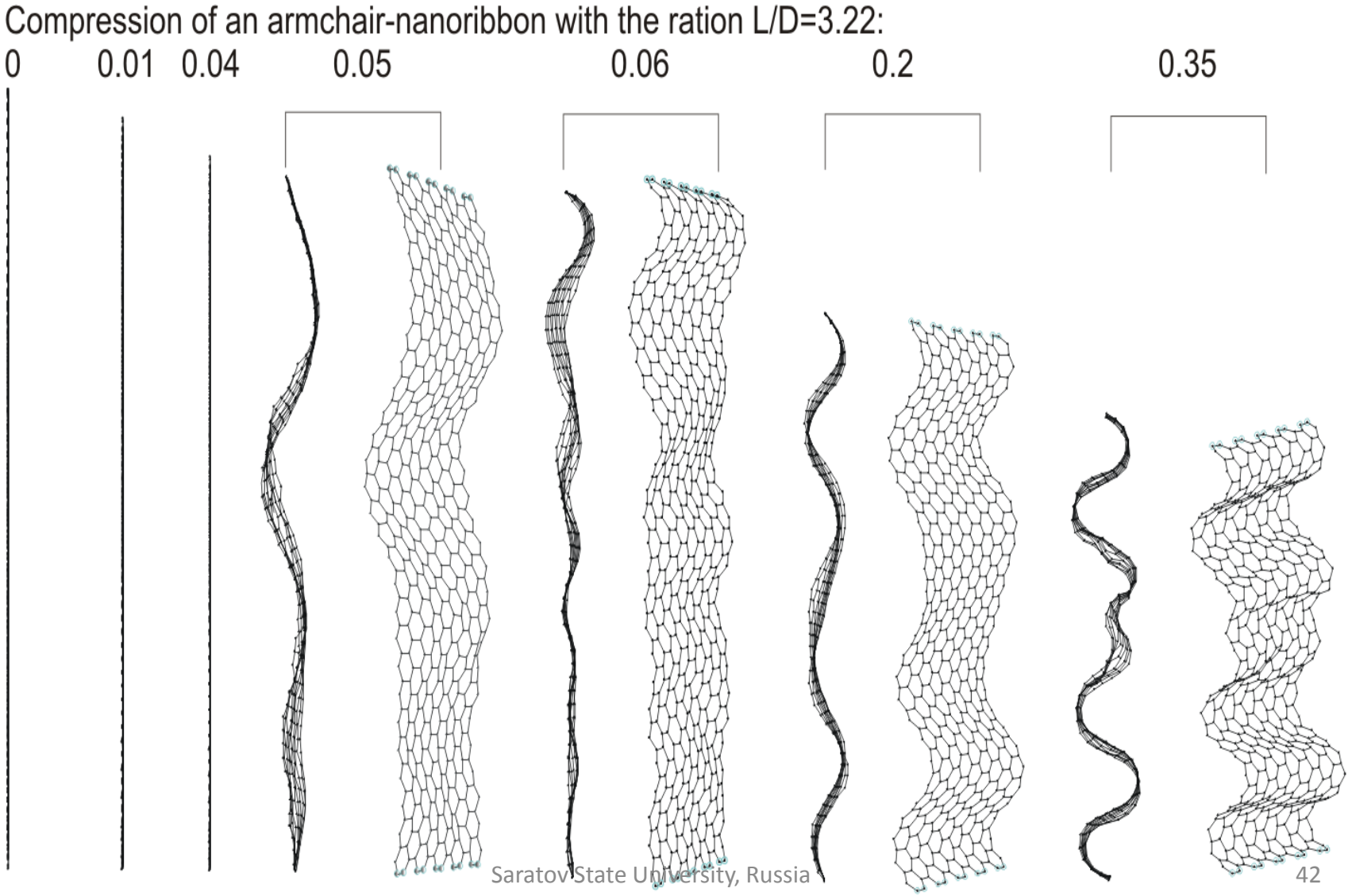

Plane network undergoing axial compression becomes wave-like. This is, so called, a phase transition.

Calculation of density of states demonstrates absence of changes in electronic structure.

However, the topology has nonzero pyramidalization angles.

Amplitude of a wave and its period are not constant and change along axis.

pyramidalization angles

$\theta_p = \theta_{\sigma\pi} - \pi/2$

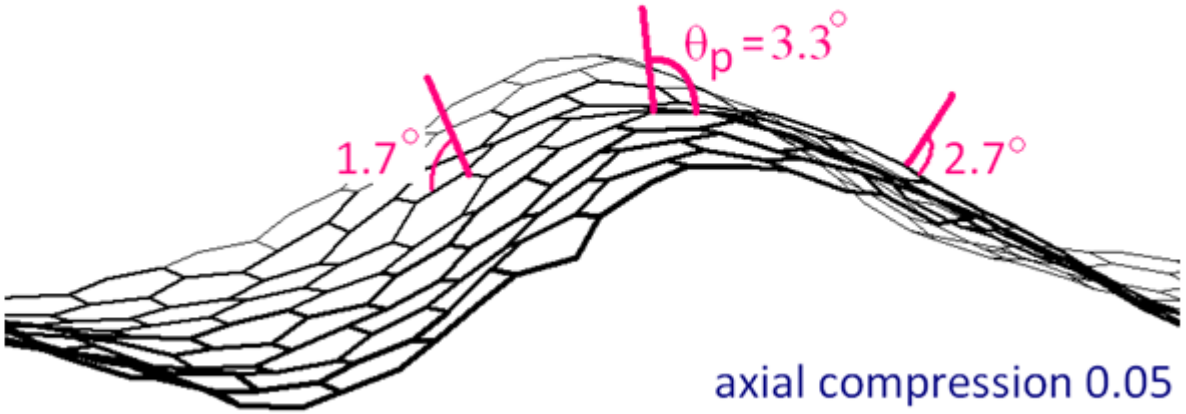

Dependency of the strain energy on the relative compression nanoparticles

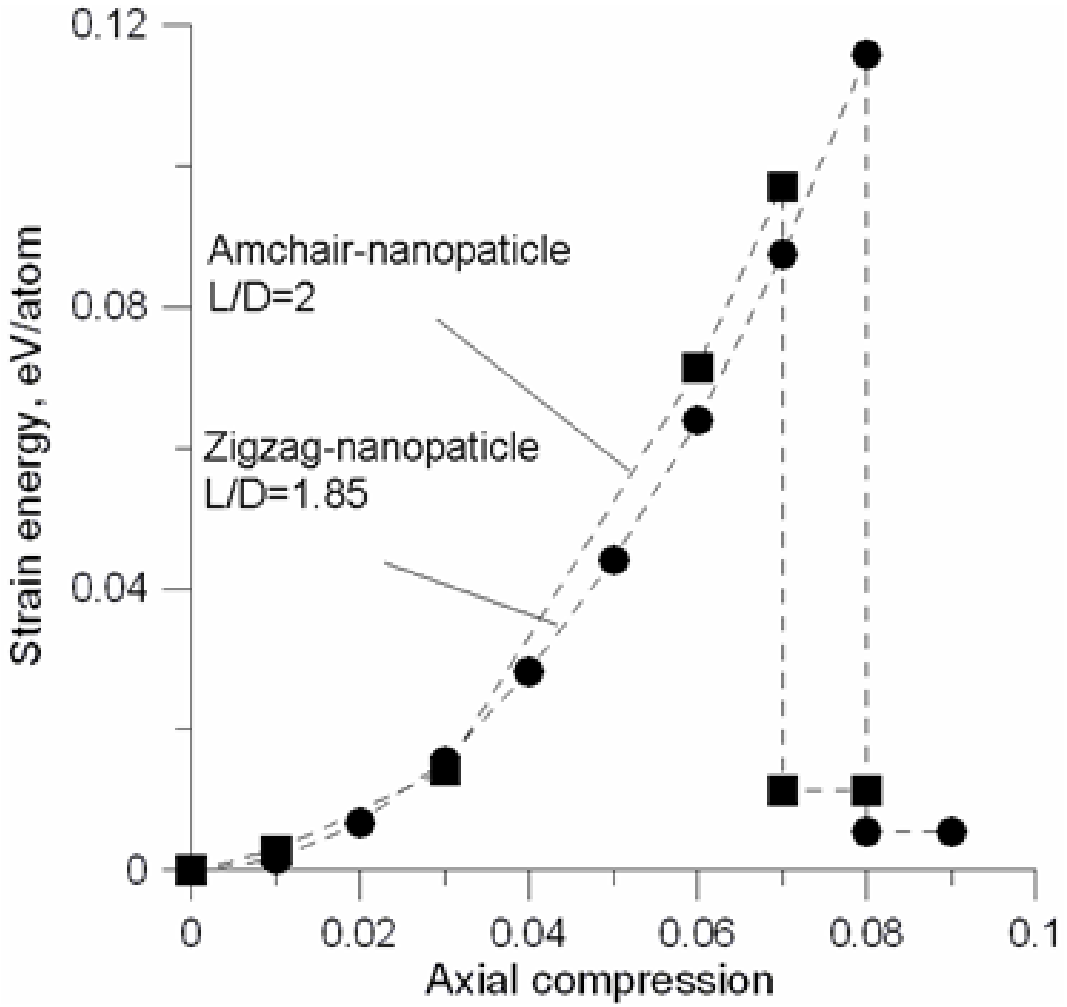

THE INFLUENCE OF A CURVATURE ON THE PROPERTIES OF NANORIBBONS

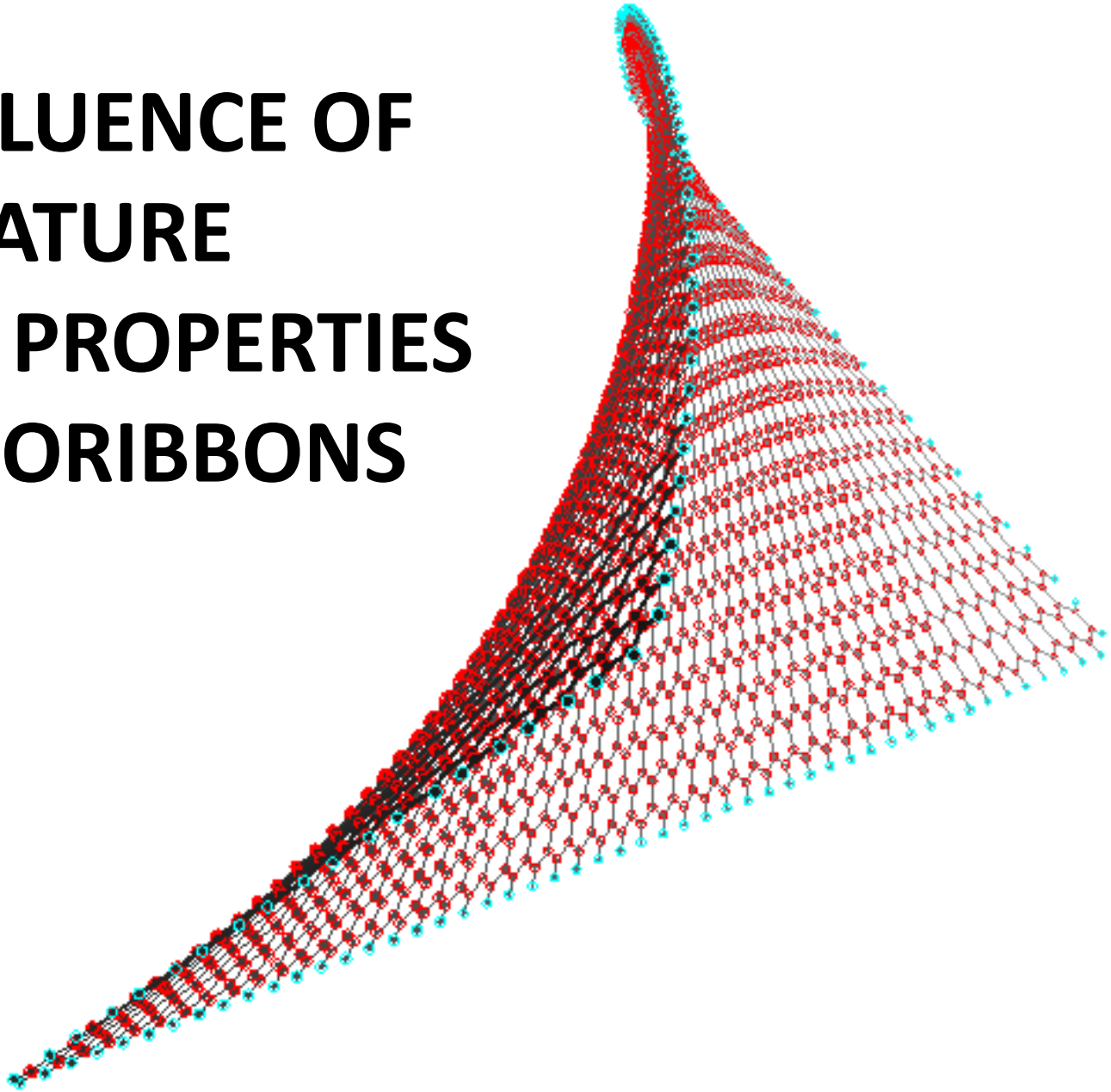

Research of the local stress field of the atomic grid of graphene nanoribbons and prediction of the appearance of defects in compression process

A new technique of calculation of the local stress fields of the atomic grid of graphene nanoribbons has been developed. The equilibrium atomic structure of nanoribbon till and in deformation process is calculated by the tight-binding method; the stress field of the atomic skeleton is calculated by the method of atom-atom Brenner potentials. The magnitude of stress near atom i is determined in a difference of the volume densities of energy of the atoms before and after deformation:

$$\sigma_i = u_i^0 - u_i = \left(\sum_{j(\neq i)} \left(V_R(r_{ij}) - B_{ij} V_A(r_{ij}) \right) + \sum_{j \neq i} \left(\sum_{k \neq i,j} \left(\sum_{l \neq i,j,k} V_{tors}(\omega_{ijkl}) \right) \right) + \sum_{j(\neq i)} V_{vdW}(r_{ij}) \right) \Big/ V_i ,$$

where the first sum – the binding energy of the atom i with the nearest-neighbor atoms chemically interacting with the atoms, the second sum – the torsion energy, the third sum – the energy of the Van-der-Vaals interaction of the atom i with the long-range atoms. Here u_i^0 – the pressure experienced by the atom i in the atomic grid in absence of deformations, u_i – the atom pressure in the deformable structure, V_i – the volume occupied by the atom.

The compression of defected nanoribbons

The comression process of graphene nanoribbons accompanied by a phase transition from plane to wave-like atomic grid has been researched. The conditions of the appearance of defects (atom vacancies) have been established and dependence of compressibility of nanoribbon from number and distribution topology of defects has been revealed by the analysis of the calculated local stress fields.

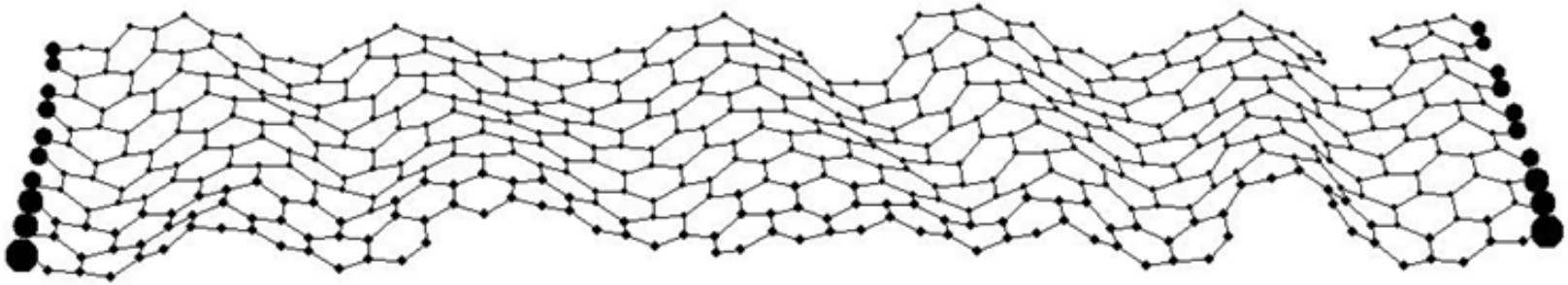

Nanoribbon compressed by 13%

The distribution of the local stress in atomic network

(the compression 20 %)

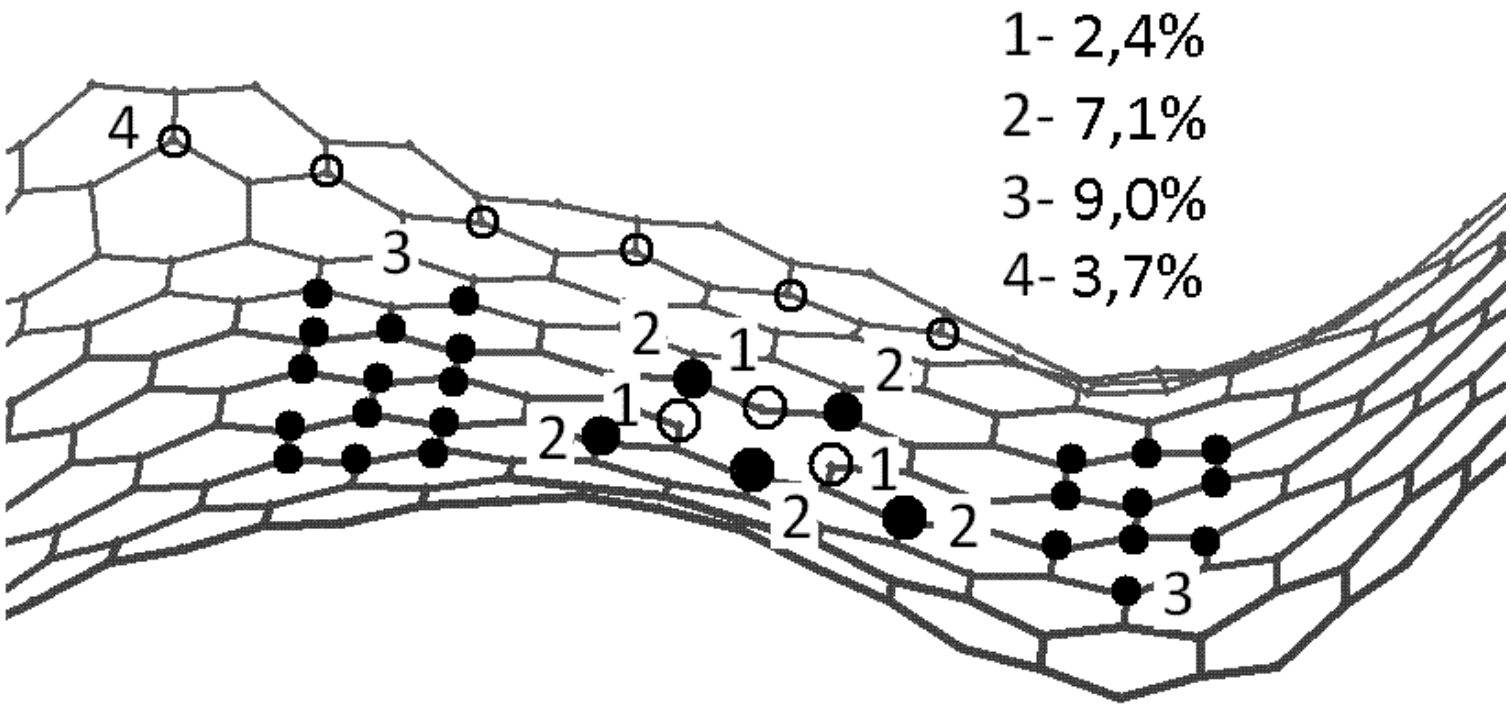

The absorption of H-atom on the atomic network

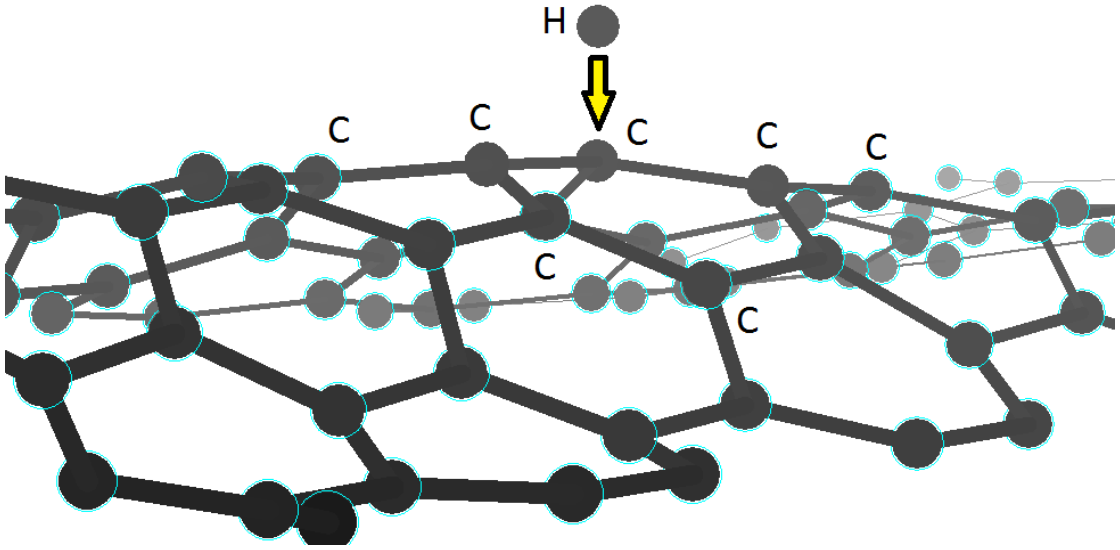

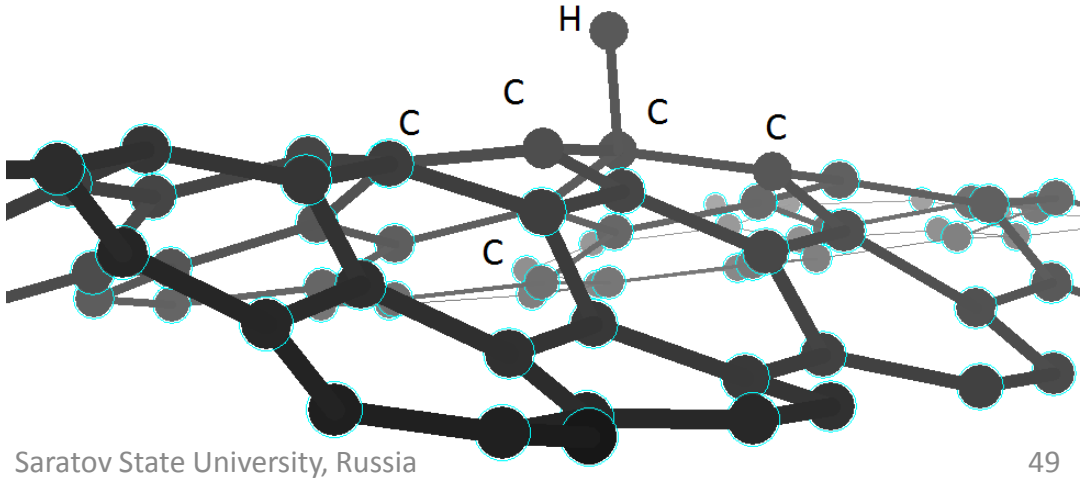

The total energy of the structure depends on the distance between the hydrogen atom and the carbon atom.

(The dashed line is the interaction of the hydrogen atom with planer graphene nanoribbon; the solid line is the interaction of the hydrogen atom from wave-like graphene nanoribbon)

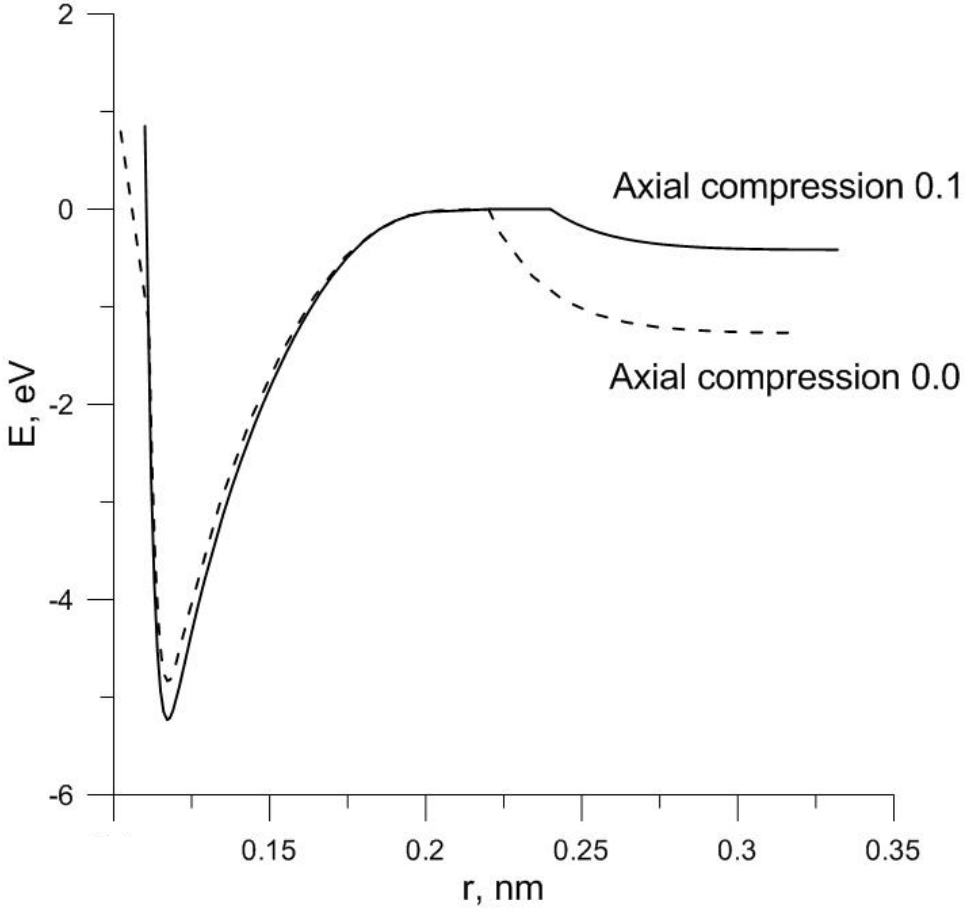

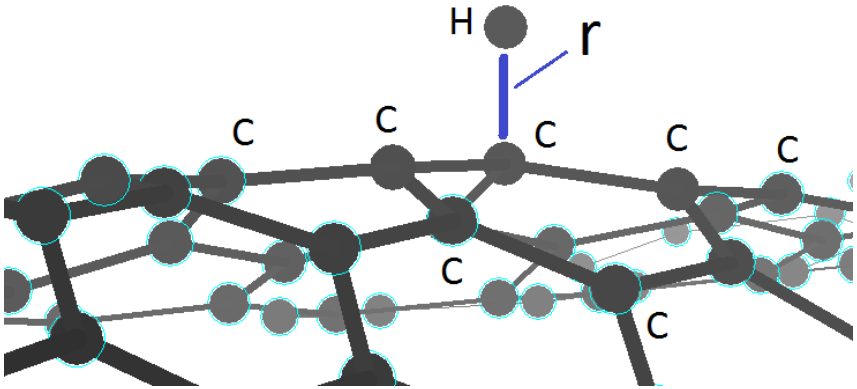

THE ELECTRON AND MECHANICAL PROPERTIES OF THE MODIFIED GRAPHENE NANORIBBONS

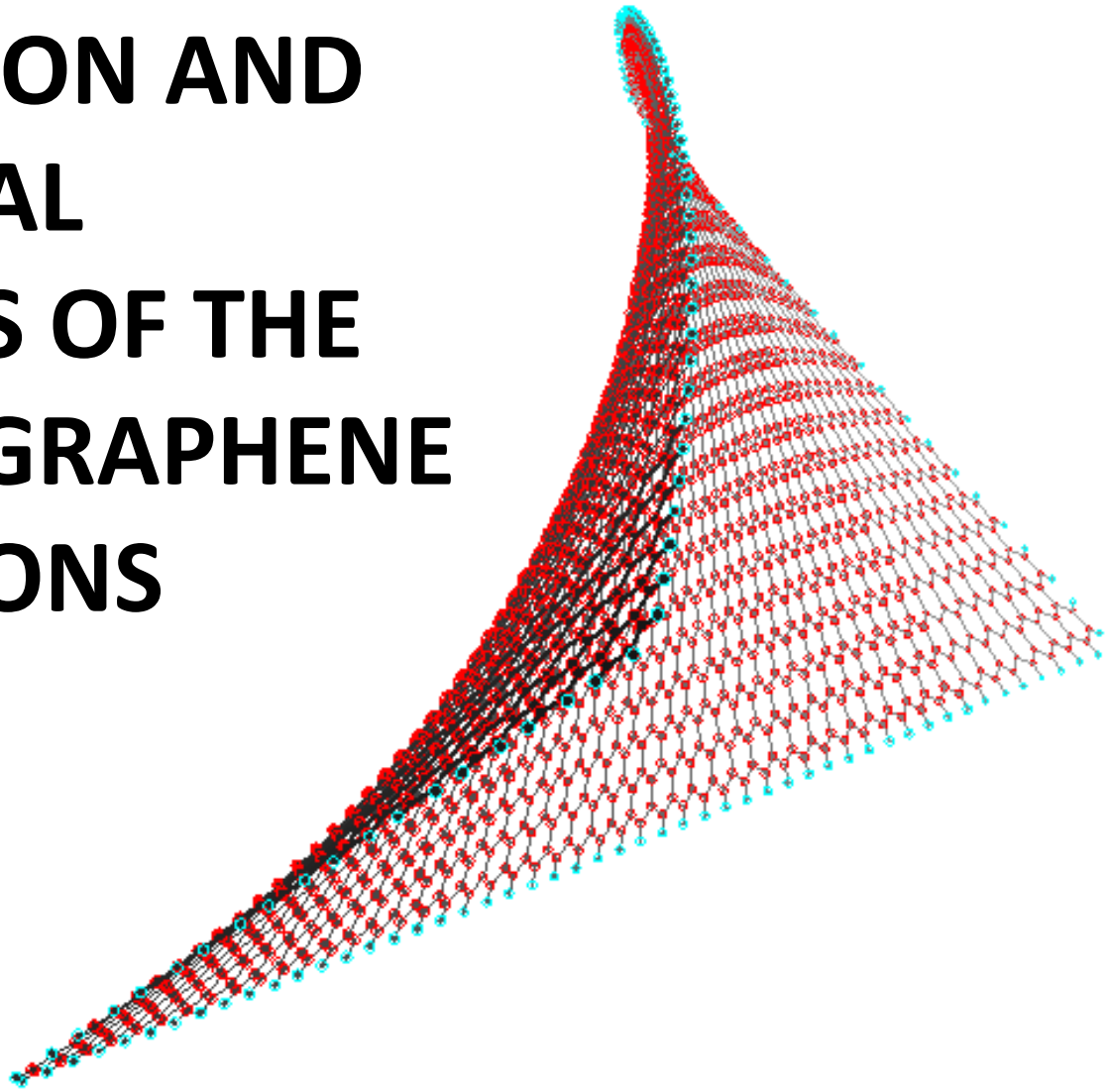

Graphane

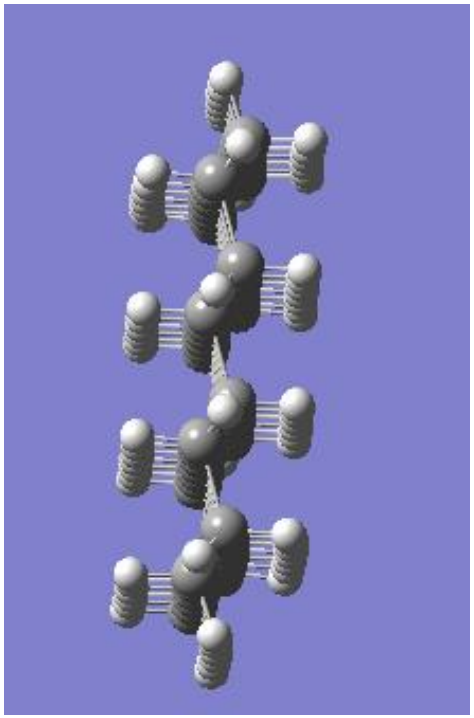

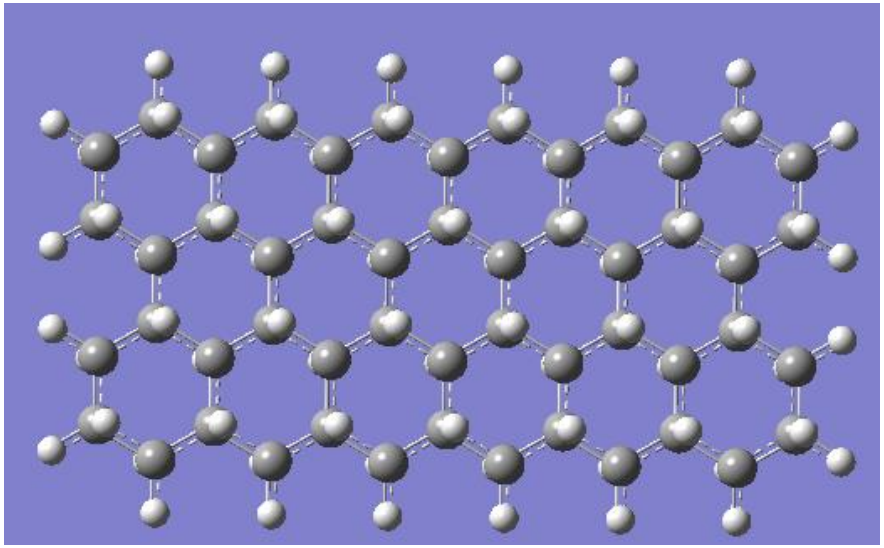

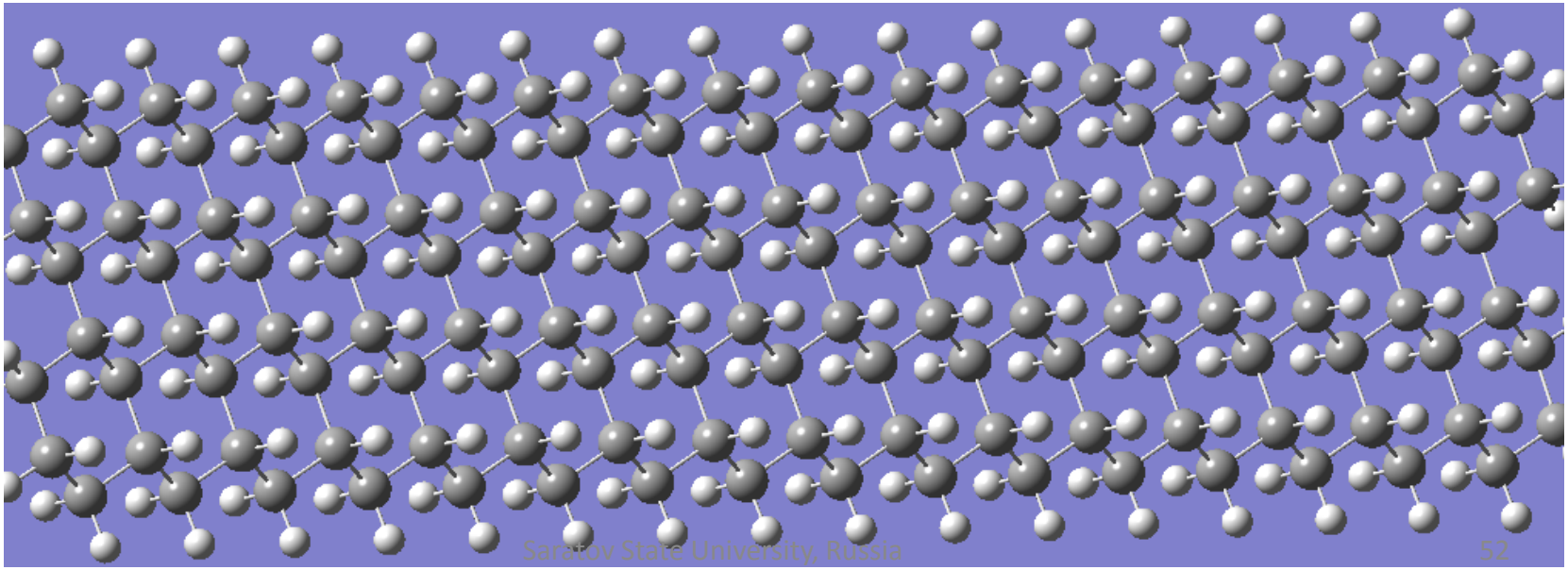

The electron properties

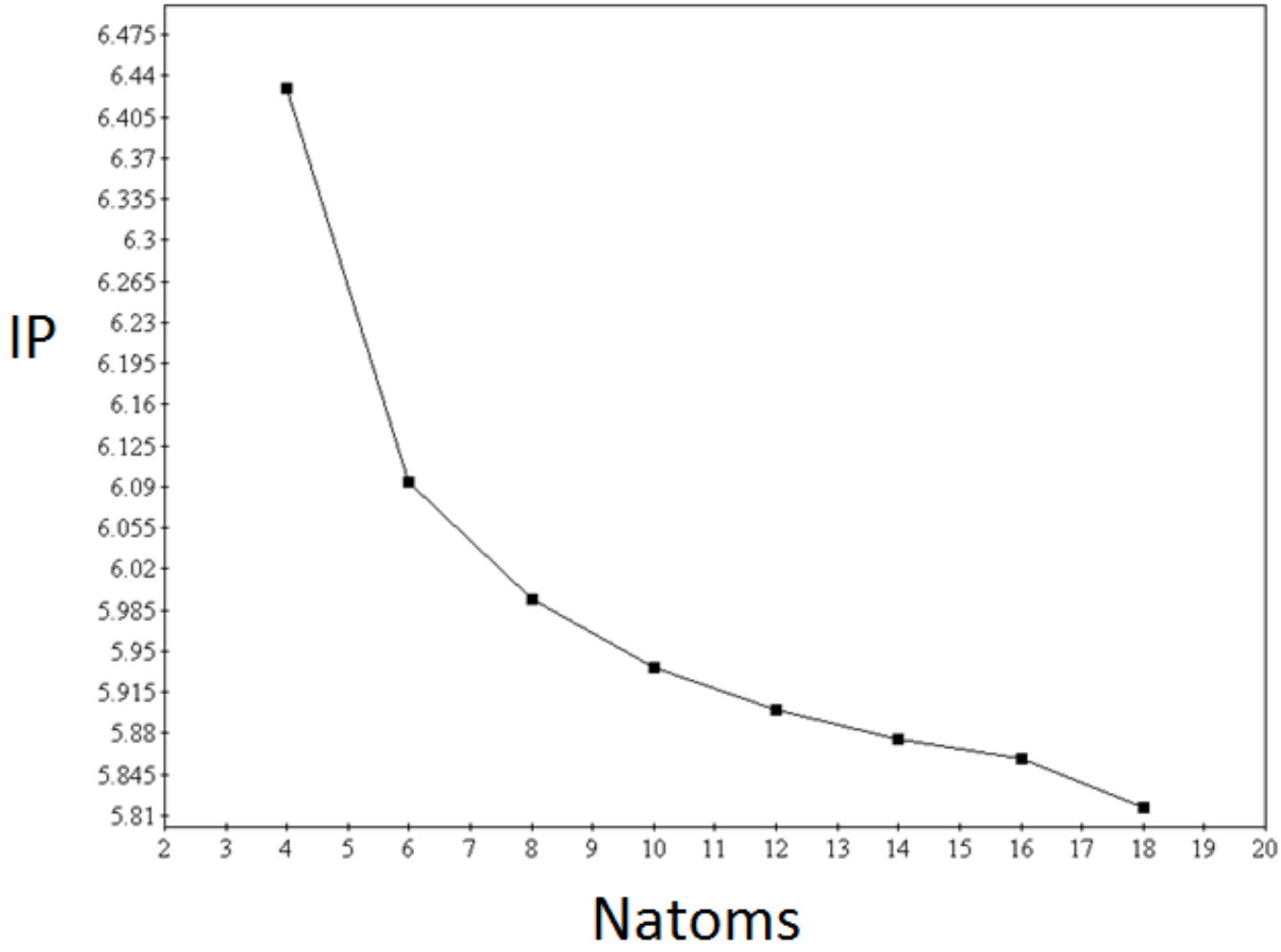

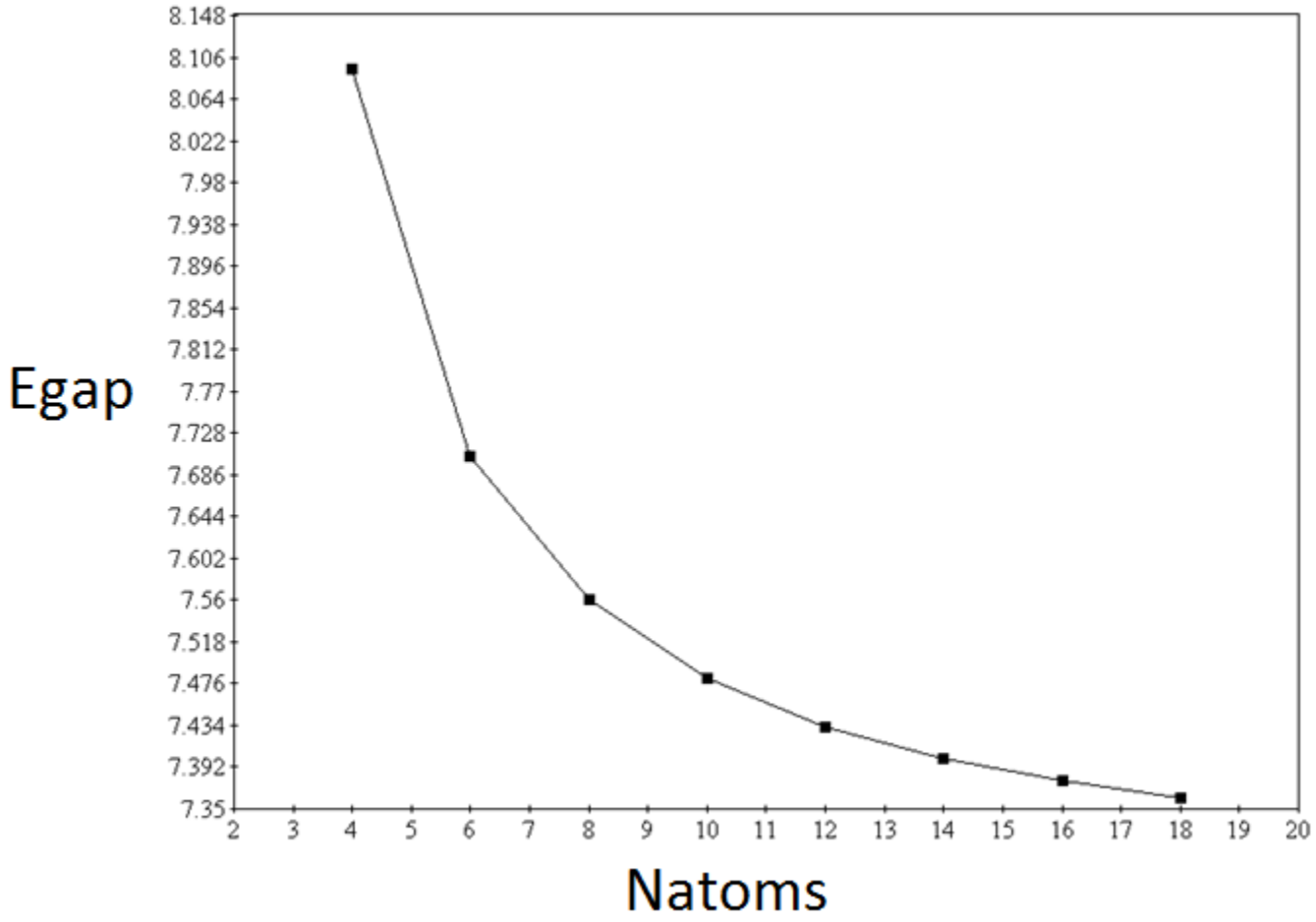
Egap
8.148
8.106
8.064
8.022
7.98
7.938
7.896
7.854
7.812
7.77
7.728
7.686
7.644
7.602
7.56
7.518
7.476
7.434
7.392
7.35
2 3 4 5 6 7 8 9 10 11 12 13 14 15 16 17 18 19 20
Natoms

Parameters of elasticity of graphane-nanostructures

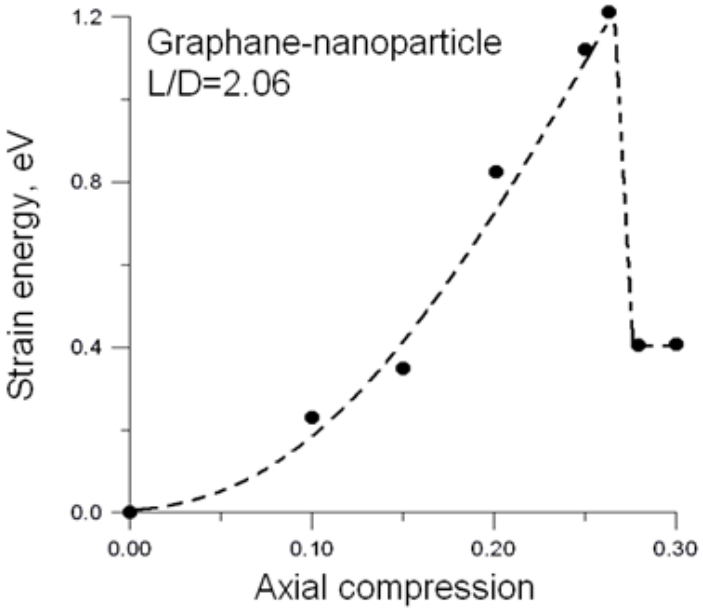

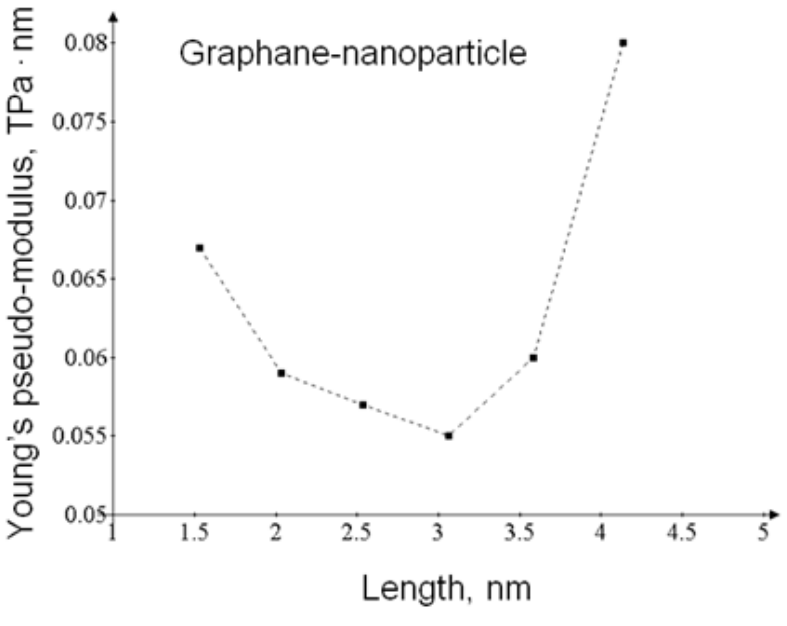

100 %

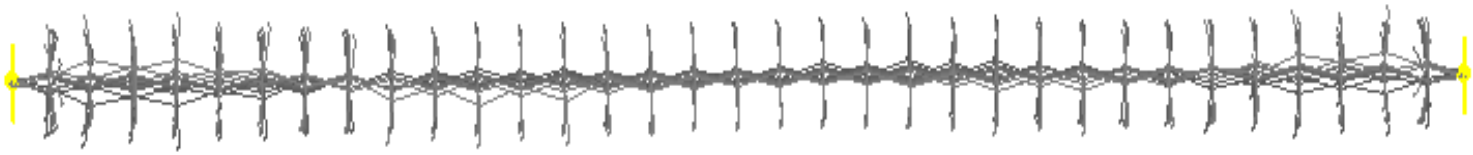

99 %

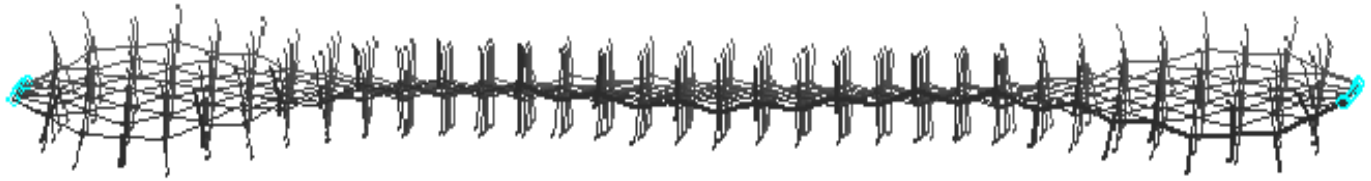

97 %